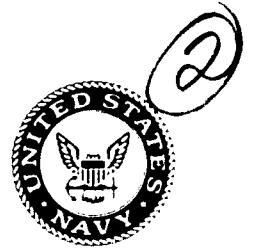


Naval Research Laboratory

Washington, DC 20375-5000



NRL Memorandum Report 6861

AD-A240 654


High Pressure Turbine Blade Life Extension

H. H. SMITH AND D. J. MICHEL

*Physical Metallurgy Branch
Materials Science and Technology Division*

August 28, 1991



91-11223



REPORT DOCUMENTATION PAGE			Form Approved OMB No 0704-0188		
Public reporting burden for this collection of information is estimated to average 1 hour per response, including the time for reviewing instructions, searching existing data sources, gathering and maintaining the data needed, and completing and reviewing the collection of information. Send comments regarding this burden estimate or any other aspect of this collection of information, including suggestions for reducing this burden, to Washington Headquarters Services, Directorate for Information Operations and Reports, 1215 Jefferson Davis Highway, Suite 1204, Arlington, VA 22202-4302, and to the Office of Management and Budget, Paperwork Reduction Project (0704-0188), Washington, DC 20503.					
1. AGENCY USE ONLY (Leave blank)	2. REPORT DATE 1991 August 28	3. REPORT TYPE AND DATES COVERED Final			
4. TITLE AND SUBTITLE High Pressure Turbine Blade Life Extension			5. FUNDING NUMBERS		
6. AUTHOR(S) H. H. Smith and D. J. Michel					
7. PERFORMING ORGANIZATION NAME(S) AND ADDRESS(ES) Naval Research Laboratory Washington, DC 20375-5000			8. PERFORMING ORGANIZATION REPORT NUMBER NRL Memorandum Report 6861		
9. SPONSORING/MONITORING AGENCY NAME(S) AND ADDRESS(ES) Naval Aviation Depot North Island San Diego, CA 92135-5000			10. SPONSORING/MONITORING AGENCY REPORT NUMBER		
11. SUPPLEMENTARY NOTES					
12a. DISTRIBUTION/AVAILABILITY STATEMENT Approved for public release; distribution unlimited.			12b. DISTRIBUTION CODE		
13. ABSTRACT (Maximum 200 words) <p>The metallurgical basis for an extension of the service lifetime of directionally solidified René 80H HPT blades beyond the rated lifetime of 30,000 EFTC was studied. The study considered the effects of HIP processing and blade tip replacement via welding with MERL 72 on the microstructure of directionally-solidified René 80H (DS-R80H) superalloy blades. Elevated temperature tensile and creep-rupture studies were conducted with DS-R80H specimens prepared from directionally solidified alloy test bars to ascertain the stress-strain and strain-time relationships and to evaluate microstructural characteristics at elevated temperatures under applied stresses. Included in the creep tests were DS-R80H specimens into which center sections of MERL 72 were inserted to evaluate the effects of stress at elevated temperature on the DS-R80H/MERL 72 interfacial integrity. In addition, the investigation considered the microstructure of MERL 72 re-tipped HPT blades following exposure of the blades in an ASMET (Accelerated Service Maintenance Engine Test) engine.</p>					
14. SUBJECT TERMS Tensile strength Creep-rupture strength Mechanical properties			15. NUMBER OF PAGES 48		
			16. PRICE CODE		
17. SECURITY CLASSIFICATION OF REPORT UNCLASSIFIED			18. SECURITY CLASSIFICATION OF THIS PAGE UNCLASSIFIED	19. SECURITY CLASSIFICATION OF ABSTRACT UNCLASSIFIED	20. LIMITATION OF ABSTRACT UL

CONTENTS

INTRODUCTION 1

MATERIALS 2

EXPERIMENTAL PROCEDURES 3

METALLOGRAPHIC RESULTS 4

TENSILE AND CREEP-RUPTURE TEST RESULTS 7

SUMMARY AND CONCLUSIONS 10

ACKNOWLEDGMENTS 12



Accession For	
NTIS GRA&I	<input checked="" type="checkbox"/>
DTIC TAB	<input type="checkbox"/>
Unannounced	<input type="checkbox"/>
Justification	
Distribution/	
Availability Codes	
Dist. Special	
A-1	

HIGH PRESSURE TURBINE BLADE LIFE EXTENSION

INTRODUCTION

Conventionally cast nickel-base superalloy turbine blades are known to exhibit limited lifetimes as the result of time-dependent plastic deformation at elevated temperatures. The deformation modes which occur at the stresses and temperatures typical of engine operation include both grain boundary sliding and cavity formation. These deformation modes are frequently responsible for a premature degradation of blade performance leading to blade replacement and to increased costs. However, hot isostatic press (HIP) processing has been used with some success to reverse the degradation produced by boundary sliding and cavity formation.

Directional-solidification techniques have been developed to optimize the elevated temperature, time-dependent strength properties of superalloys. In particular, the orientation of the cast grain boundaries parallel to the axis of the turbine blade during directional solidification virtually eliminates both grain boundary sliding and cavity formation as active deformation modes during elevated temperature service. However, time dependent deformation of the alloy does occur by other mechanisms leading to eventual degradation of the turbine blades.

The high-performance F404 gas turbine engine in the F-18 aircraft was originally equipped with conventionally cast René 125 high pressure turbine (HPT) blades rated at a life of 15,000 EFTC (Effective Full Thermal Cycles). An engineering change involving the replacement of the HPT blades with directionally solidified René 80H (DS-R80H) was made to provide a blade lifetime of 30,000 EFTC.

The purpose of this investigation was to evaluate the metallurgical basis for extending the service lifetime of directionally solidified René 80H HPT blades beyond the rated lifetime of 30,000 EFTC. The study considered the effects of HIP processing and blade tip replacement via welding with MERL 72 on the microstructure of directionally-solidified René 80H (DS-R80H) superalloy blades. Elevated temperature tensile and creep-rupture studies were conducted with DS-R80H specimens prepared from directionally solidified alloy test bars to ascertain the stress-strain and strain-time relationships and to evaluate microstructural characteristics at elevated temperatures under applied stresses. Included in the creep tests were DS-R80H specimens into which center sections of MERL 72 were inserted to evaluate the effects of stress at elevated temperature on the DS-R80H/MERL 72 interfacial integrity. In addition, the investigation considered the microstructure of MERL 72 re-tipped HPT blades following exposure of the blades in an ASMET (Accelerated Service Maintenance Engine Test) engine.

MATERIALS

HIGH PRESSURE TURBINE BLADES

DS-R80H HPT blades, both new and those removed from F404 engines after 14,030 EFTC (low EFTC) and 27,449 EFTC (high EFTC), were received from the NADEP NORIS for evaluation in this study. All blades received a CODEP coating and the precipitation heat treatment as shown in Table 1. Additional blades in all three conditions were received from NADEP NORIS, via Chromalloy Division Oklahoma, following removal of the CODEP coating. Figure 1 illustrates the appearance of the HPT blades without the CODEP coating. The severe erosion of tip region of both the low and high EFTC blades is readily apparent in Figure 1.

TIP REPAIRED HPT BLADES

New, low and high EFTC engine run blades were supplied by NADEP NORIS to Chromalloy Division Oklahoma for trial blade tip repair using the MERL 72 alloy. Selected blades were cleaned of the CODEP coating and sectioned to remove the original blade tip region. The MERL 72 alloy was then weld deposited on the blade by Chromalloy Division Oklahoma to reconstruct the blade tip region. The blades then received the precipitation treatment in Table 1. Selected re-tipped blades were sent to NRL for metallographic evaluation while the remaining blades were retained for ASMET engine testing.

ASMET ENGINE TEST BLADES

NRL was supplied with eight (8) MERL 72 tip repaired DS-R80H HPT blades and two (2) new blades following an ASMET engine run. These blades were operated in the test engine for 150 ASMET hours. The correlation between ASMET hours and flight hours is 3.33:1; therefore, the blades were subjected to approximately 500 simulated flight hours of thermal cycling. The corresponding value of the equivalent full thermal cycles (EFTC) experienced by the blades in the ASMET engine test is 4656. For the tip repaired blades, the ASMET engine exposure was in addition to previous unrecorded engine histories.

DS-R80H TENSILE AND CREEP-RUPTURE SPECIMENS

Directionally solidified René 80H material was received from Howmet Turbine Components Corporation in the form of 7 mm diameter (approximately one-quarter inch diameter) rods. Tensile and creep-rupture specimens with the dimensions shown in Figure 2 were prepared from the rods. The alloy compositions and the precipitation treatment given the specimens prior to testing are given in Table 1.

DS-R80H/MERL 72/DS-R80H CREEP-RUPTURE SPECIMENS

The creep-rupture behavior of combined MERL 72 weld/DS-R80H specimens was investigated using test specimens of DS-R80H which were modified to remove a portion (5 mm in length) of the gage section and insert a weld zone of MERL 72. The specimens were then re-contoured to the dimensions in Figure 2 and re-heat treated according to Table 1 prior to creep-rupture testing.

EXPERIMENTAL PROCEDURES

METALLOGRAPHIC PROCEDURES

Selected HPT blades were sectioned to examine blade tip erosion, cracking, weld repair characteristics and weld microstructures. Conventional metallographic procedures were employed to prepare the blade sections for optical study. The polished sections were etched in a solution of 5 gm of CuCl_2 , 100 ml of HCl and 100 ml of ethanol prior to optical and electron microscopic examination. Fractographic analyses of the HPT blade cracks and of the test specimen fracture surfaces were performed using scanning electron microscopy (SEM). Semi-quantitative energy dispersive x-ray analyses were performed using the SEM to determine composition profiles across matrix/weld interfaces. Thin foil specimens of the DS-R80H blade material were prepared by twin-jet electrochemical thinning for examination by transmission electron microscopy (TEM).

HIP PROCESSING

Selected new, low and high engine run blades and creep-rupture test specimens were HIP processed by Chromalloy Division Oklahoma. The HIP parameters are given in Table 1. These tests were conducted to evaluate the applicability, if any, of HIP processing to recover non-surface connected internal creep porosity developed in these blades during engine operation.

TENSILE AND CREEP-RUPTURE TESTING

Tensile and creep-rupture tests of the precipitation heat treated and/or HIP processed DS-R80H alloy test specimens were conducted at 871 and 982°C (1600 and 1800°F). These temperatures represent thermal conditions at and above the final aging temperature of the DS-R80H blade prior to entering service. The stress levels selected for creep-rupture testing were determined from the tensile test results and from the computed blade profile parameters reported in F404 engine design documents. Creep strains were measured with an linear variable displacement transducer (LVDT) extensometer attached to the specimen grips during testing.

METALLOGRAPHIC RESULTS

NEW AND ENGINE-RUN HPT BLADES

The optical microstructure of a new DS-R80H blade is illustrated in Figure 3. Note the columnar (directional) orientation of the grains parallel to the axis of the blade in Figures 3b and 3d. The microstructural appearance of the alloy at a higher magnification is shown in Figure 3a. In this figure, the carbide phase (white globules) and the gamma prime strengthening phase (faint background) are visible.

The microstructure of the engine run and new blades is illustrated in Figure 4. This figure compares the microstructure of the blades at two locations along the blade axis. In the mid region of the blades, approximately the mid-point of the length of the blade, the microstructure of all three blades is seen to be similar.

The gamma prime precipitate microstructure of a new HPT blade is compared with the equivalent microstructure of a heat treated, but untested, creep-rupture specimen in Figure 5. Neither the blade nor the test specimen was HIP processed prior to the precipitation heat treatment. As is readily evident from the micrographs, the precipitate size and density of both the blade and the test specimen are essentially identical.

HIP PROCESSED HPT BLADES

The effect of hot isostatic press (HIP) processing on the microstructure of the new and engine-run blades was investigated. Figure 6 illustrates that the microstructures of the mid region of the HIP processed and not-HIP processed blades was similar for all three blade life conditions examined. However, as shown in Figure 7, the microstructure of the tip region of the not-HIPped low and high EFTC blades have experienced considerable coarsening of the gamma prime precipitate when compared with the microstructure of the new blade in this location. Following HIP processing, all three blades have been restored to a similar microstructural condition.

Figure 8 compares the gamma prime precipitates in the tip region of the low and high EFTC blades both prior to and following HIP processing. Prior to HIP processing, the gamma prime precipitate size and spacing are non-uniform suggesting that partial precipitate dissolution has been experienced by the material. For both blade conditions, the effect of HIP processing has been to restore uniformity to the precipitate size and spacing which contributes to the elevated temperature creep strength of the alloy.

TIP REPAIRED HPT BLADES

The blade tip erosion visible in Figure 1 and the microstructural examination of the engine run blades suggested that a blade tip repair procedure could be considered to extend the blade life since the structure of all blades below the tip regions exhibited no apparent degradation from F404 engine operation. Chromalloy Division Oklahoma suggested the use of MERL 72, a cobalt-base alloy, as a possible tip repair material on the basis of previous blade tip repair experience. Subsequently, Chromalloy Division Oklahoma produced trial blade tip weld repairs using MERL 72 on both low and high EFTC blades for NRL evaluation.

Figure 9 shows the optical microstructure of the interior and exterior surfaces of a DS-R80H blade which has undergone the MERL 72 blade tip repair. Note the appearance of the interface between the directionally solidified grains and the weld deposited material. Figure 10 shows section views of the blade illustrating the well-defined blade-weld interface at several locations. Note the clearly defined interface between the weld and the blade alloy at all sections. However, in sections 2 and 8, small discontinuities originating from the blade interior are clearly visible. These are thought to be associated with oxidation products remaining from the prior engine operation.

The microstructure of the blade-weld interface is illustrated in the optical micrographs in Figure 11. Figure 11a shows that the weld deposit has formed a porosity-free metallurgical bond with the blade alloy, with minimal dissolution of the blade alloy microstructure. Figures 11(b) through (d) illustrate the microstructures of the blade, weld fusion zone and weld, respectively. In particular, the microstructure of the weld fusion zone shows that minimal dissolution of the blade alloy has occurred during the welding process and that the heat-affected zone was confined to the narrow region near the blade/weld interface.

The composition profiles of nickel, chromium and cobalt through the blade-weld interface are shown in Figure 12. The profiles confirm that minimal intermixing of the blade and weld alloys occurred during the tip repair process. Additional detail of the microstructure of the blade/weld interface is illustrated by the TEM micrographs in Figure 13. The micrographs show the change in the microstructure from the blade alloy to the weld as the interface was traversed. The micrographs clearly show the minimal intermixing of the blade and weld alloys which occurred during the blade tip repair process.

ASMET ENGINE TESTED HPT BLADES

The blade tip regions of the HPT blades which were ASMET engine tested are illustrated in Figure 14. Note the physical condition, especially the trailing edge tip of each blade, which

shows the erosion and/or cracking produced by the ASMET engine test exposure. In particular, note the severe erosion of the blade which was new prior to the engine test and the general lack of erosion of the tip repaired blade with a similar cooling hole configuration.

Figure 15 shows the microstructure of a new HPT blade after ASMET engine testing. The severe trailing edge tip erosion is shown in Figures 15(a) and (b). Figures 15(c) and (d) show the development of cracking along grain boundaries. The coating/matrix interaction is shown for both the blade tip and the blade face in Figures 15(e) and (f).

The microstructure of an engine run HPT blade (total EFTC unknown) which was MERL 72 weld tip repaired by Chromalloy Division Oklahoma, configured with the original cooling hole scheme and ASMET engine tested is shown in Figure 16. Figures 16(a) and (b) illustrate a crack which developed at the blade surface which followed the DS-R80H/MERL 72 interface. Figure 16(c) shows the crack tip region and the oxide formed along the entire crack path. Figures 16(d), (e) and (f) illustrate the microstructure of the coating/weld and coating/matrix interactions at various locations on the HPT blade.

A portion of an ASMET engine tested blade which contained a crack in the repaired blade tip was fractured at liquid nitrogen temperatures to separate the crack and to reveal the details of the crack surfaces. The fractographs in Figure 17 relate to a tip repaired to the original tip cooling scheme. The darker, oxidized crack surfaces were generated by processes during the ASMET engine run and the lighter surfaces were formed when the crack was fractured open. Cracking appears to have initiated at the cooling hole, Figure 17(c), and outside blade surfaces. The crack eventually assumed a growth direction perpendicular to the crack front shown in Figures 17(a) and 17(b).

The microstructure of an engine run HPT blade (total EFTC unknown) which was MERL 72 weld tip repaired by Chromalloy Division Oklahoma, configured with a recessed shelf tip cooling scheme and ASMET engine tested is shown in Figure 18. Figure 18(a) illustrates a crack observed in the MERL 72 weld in the vicinity of a cooling hole. Figure 18(b) shows the crack tip region at the DS-R80H/MERL 72 interface. These regions are shown in greater detail in Figures 18(c) and (d). Note the reaction zone formed within the weld along the crack surface and at the top surface of the blade tip, Figure 18(c). Of the four tip configurations examined microstructurally, only the recessed shelf tip cooling hole configuration exhibited this behavior. No differences in microstructure, weld alloy chemistry or coating integrity could be determined which would explain the formation of the reaction zone observed for this blade.

The microstructure of an engine run HPT blade (total EFTC unknown) which was MERL 72 tip repaired by Chromalloy Division Oklahoma, configured with counterbored tip cooling holes and ASMET engine tested is shown in Figure 19. Figure 19(a) illustrates the overall view of a counterbored cooling hole showing a crack which originated at the tip surface/hole interface. Figures 19(b), (c) and (d) illustrate the details of cracking in this region.

The microstructure of an engine run HPT blade (total EFTC unknown) which was MERL 72 tip repaired by Chromalloy Division Oklahoma, configured with concave side tip film cooling holes and ASMET engine tested is shown in Figure 20. Figure 20(a) illustrates the overall view of a crack associated with a cooling hole. Figure 20(b) illustrates the detail of the crack in the weld built-up blade tip. Fractographs of a crack similar to that shown in Figure 20 are shown in Figure 21. Similar to most blade tip cracks examined, the crack in Figure 21 appeared to initially propagate from the top and outside portions of the blade. The crack then grew as a through-thickness crack, with the crack tip boundary larger on the outside face of the blade.

The ASMET engine tested blades showed no metallurgical weld defects, such as cracking or porosity. Weld metal dilution effects were examined using the SEM to conduct semi-quantitative energy dispersive x-ray analyses of the blade-weld interface region. Alloy composition profiles are shown in Figure 22 for the elements Ni, Cr, Co, Ti and W. The data indicate that elemental mixing at the interface of the repair was confined to a region approximately 1 mm or less in overall extent. These results are in agreement with those found for previously repaired blades, Figure 12, and suggest that the weld repair process can be expected to be repeated with considerable consistency.

CREEP-RUPTURE TEST SPECIMENS

The microstructure of the not-HIP and HIP processed, precipitation heat treated, untested creep-rupture test specimens is illustrated in Figure 23. For both material conditions, the microstructures are seen to be equivalent indicating that HIP processing produced no observable effect on the test specimen microstructure.

TENSILE AND CREEP-RUPTURE TEST RESULTS

DS-R80H SPECIMENS

The tensile and creep-rupture test results are summarized in Table 2. The results show that creep ductility increased with increasing test temperature. Typical creep-rupture test results from the DS-R80H specimens, heat treated to include the time at temperature of the coating cycle, are shown in Figure 24 for DS-

R80H specimen material 455 tested at temperatures of 871 and 982°C (1600 and 1800°F).

To investigate the effects of HIP processing on the creep behavior of DS-R80H, creep tests of specimens from material 491 (Table 2) were interrupted during the tertiary creep stage. The specimens were then removed from the creep test machine, HIP processed and re-heat treated to the original conditions, including the time at temperature of the coating cycle. The specimens were then re-installed in the creep machines and the tests were continued to specimen failure. The results from these not-HIP/HIP processed tests at 871 and 982°C are shown in Figure 25. The horizontal lines in Figure 25 indicate the strain at which the tests were interrupted so that the specimens could be HIP processed. For the creep specimen tested at 871°C, the initial stress level was 40 ksi. At a strain level of 3%, the stress level was increased to 51 ksi. The dashed portion of the curve in Figure 25 represents the expected creep response of the specimen if the test had been conducted entirely at 51 ksi.

The results in Figure 25 show that the HIP processing provided little change to the creep response of the DS-R80H when compared with the results from the not-HIP processed creep specimens of material 491. As shown in Table 2, the combined not-HIP/HIP processed creep life of specimens of material 491 was slightly reduced from the life of the not-HIP processed specimens tested at both temperatures. In addition, the mid-test application of the HIP and heat treatment cycle reduced the specimen reduction in area and elongation values by approximately 50% when compared with the not-HIP processed condition.

Table 2 shows the effect of HIP processing on the creep behavior to two pairs of creep specimens from material 455. The specimens were all from the same heat of material, but were machined from two separate cast rods and the pairs were HIP processed separately. The data show a large disparity in creep lives which cannot be explained on the basis of either microstructure or test conditions. However, the oxide on the tested N455 specimens exhibited a different appearance than all other tested specimens. Analysis of the surface oxide on the N455 specimens by X-ray spectroscopy revealed a large nickel and aluminum peak not found for the E455 specimens. The nickel and aluminum surface concentrations suggest that the N455 specimens may have inadvertently received a coating treatment when the specimens were HIP processed. The inferior creep performance of the uncoated specimens indicates that HIP processing may severely reduce the creep life of DS-R80H at the stress levels and temperatures of this study. Nevertheless, creep ductility as reflected by the measured creep strain was comparable for the not-HIP and HIP processed materials. The differences in creep lives of the coated and uncoated specimens demonstrates the effectiveness of the coating to influence the creep lives after HIP processing.

Scanning electron microscopy (SEM) was used to examine the rupture surfaces of the creep/rupture specimens tested in this investigation. SEM micrographs from a specimen tested at 871°C (1600°F), Figures 26(a) and (c), show that both the HIP processed and non-HIP processed specimens failed in a ductile manner by microvoid coalescence. However, for the specimens tested at 982°C (1800°F), the SEM micrographs indicate evidence of surface cracking which linked up to reduce the creep life of the HIP and, to a lesser extent, the not-HIP processed specimens, Figures 26(b) and (d).

The microstructure of the creep-rupture specimens are illustrated in Figure 27. The figures show the influence of both test temperature and HIP processing on the microstructure. The micrographs show that the creep-rupture tests at a temperature of 982°C produced a partial dissolution of the gamma prime precipitates leading to increased matrix ductility and a reduced creep/rupture life. Intermediate HIP processing, as shown in the not HIP/HIP processed TEM microstructure, partially restores the gamma prime precipitate structure leading to a slight reduction in the creep rate upon resumption of the creep test as shown in Figure 25. However, the creep-rupture tests at a temperature of 871°C produced no apparent change in the gamma prime precipitate size and number density. The micrographs show that the HIP processing produced minimal benefits to both the microstructure and to the creep/rupture properties of the DS-R80H as shown by the comparison of the creep behavior in Figures 24 and 25.

The effect of HIP processing on the creep lives at both 871 and 982°C was consistent with the expectations for a directionally solidified specimen whose stress axis was coincident with the grain orientation. That is, the carefully controlled directional solidification and the absence of grain boundaries oriented near 90 degrees to the stress axis virtually eliminated the occurrence of grain boundary porosity which could be removed by HIP processing.

DS-R80H/MERL 72/DS-R80H SPECIMENS

Figure 28 illustrates the overall appearance of the DS-R80H/MERL 72/DS-R80H specimens in both the untested and creep-rupture tested conditions. Note the formation of a neck in the creep-rupture tested specimen indicative of the extent of ductility developed in the weld material rather than in the blade/weld interface.

The creep-rupture results for the blade/weld specimens at 871°C are shown in Figure 29 and are given in Table 2. When compared with the results for the blade alloy, Figure 24 and Table 2, the results show that the creep life of the MERL 72 weld was drastically reduced from that exhibited by the DS-R80H. For example, the results show that at a stress level of 51 ksi, the

creep life of the MERL 72 was 1.3 hours compared with 289 hours for the DS-R80H. Similar reductions in the creep lives of the MERL 72 occurred at the lower stress levels. The appearance of the fracture surfaces of the MERL 72 creep-rupture specimens is shown in Figure 30. The micrographs show that the fracture surface exhibited microvoid coalescence which was consistent with the high level of ductility observed in the weld material. The results confirm that the weld material exhibited ductility levels consistent with the maintenance of the integrity of the blade/weld interface in the test specimens.

SUMMARY AND CONCLUSIONS

The objective of this study was to develop the metallurgical basis for the life extension of F404 HPT blades beyond 30,000 EFTC. Examination of engine-run HPT blades revealed that the blade tip region was severely eroded by the combined effects of the elevated temperature exposure, the blade tip-shroud contact and the flow of cooling air exiting the blade tip. The alloy microstructure in the vicinity of the blade tip showed the partial dissolution of the gamma prime strengthening precipitate phase which indicated that the blade tip areas experienced temperatures above 871°C (1600°F) and perhaps above 982°C (1800°F). Further investigation of the engine-run blades suggested that repair of the eroded tip region through the use of a weld-deposited MERL 72 could provide the basis for the extension of the blade life, provided that creep strength of the weld material was not a limiting factor.

The tensile and creep-rupture test results have demonstrated that the directionally solidified R80-H alloy exhibited deformation at the temperatures and stress levels typical of the blade service environment without the development of intergranular porosity. The results suggest that the use of HIP processing to eliminate the creep porosity will be unnecessary and that such HIP processing may not provide a beneficial increase in creep life. Creep-rupture tests of DS-R80H specimens into which a MERL 72 weld zone was inserted demonstrated the interfacial integrity of the blade/weld region and that the creep strength of the weld was maintained at the 871°C test temperature.

A demonstration of the feasibility of the proposed MERL 72 welded tip repair process was provided by an ASMET engine test. Microstructural examination of the ASMET engine tested blades revealed that the overall integrity of the blade/weld interface was unaffected by the engine exposure. Further, the examination showed that trailing edge tip crack formation only occurred in the vicinity of the blade tip cooling holes. The examination revealed that the weld repaired blade tips exhibited superior resistance to erosion during the ASMET engine test when compared to the new DS-R80H blades. The side tip film and recessed shelf tip cooling schemes were effective in reducing cracking on the high pressure

blade surfaces, but cracking occurred on the low pressure faces associated with tip cap cooling holes. In addition, it was observed that the weld repaired blade tips with the recessed shelf, counterbored hole and concave side tip film cooling hole schemes exhibited little evidence of shroud contact during the ASMET engine test.

Based on all technical results developed during the course of this study, there appears to be no known basis, from a materials viewpoint, to limit the life of the DS-R80H HPT blades in the F404 engine. However, additional information, as yet unknown to the authors, may provide the basis for a life limit.

Within the scope of this study, the following conclusions can be drawn from the experimental results which were obtained:

1. The erosion of the trailing edge of the HPT blades examined is concluded to result from the combined effects of tip temperatures in excess of 871°C, shroud contact and cooling air flow.
2. The application of HIP processing to restore the original precipitation strengthened DS-R80H microstructure is concluded to be desirable. However, the effect of the HIP processing on DS-R80H HPT blade life is unknown, and may be adversely affected as demonstrated by creep-rupture test results.
3. The repair of DS-R80H HPT blade tip regions by weld deposit of MERL 72 is concluded to be feasible on the basis of microstructural studies of repairs both prior to and following ASMET engine tests.
4. The extension of HPT blade life via the weld deposit of MERL 72 on DS-R80H blades is concluded to be feasible for one repair cycle as demonstrated by the limited duration ASMET engine test results. However, the technical evidence required to show that the weld tip repair is feasible for additional repair cycles has not been obtained.

Several unresolved issues with regard to the HPT blades still remain to be addressed. These are:

1. The metallurgical analysis has demonstrated no discernable degradation of the HPT blades other than the blade tip regions. Therefore, what is the technical and/or materials basis for the life limit of 30,000 EFTC specified for the HPT blades?
2. Would new DS-R80H HPT blades benefit from welded tips prior to engine installation?
3. What are the effects of overtemperature (i.e. above 1000°C) on the gamma prime precipitate microstructure; are the time - temperature - gamma prime kinetics known for R80H?

ACKNOWLEDGMENTS

The authors wish to thank Mr. Bob France, NADEP NORIS, for his suggestions which led to this investigation and for his enthusiastic support throughout the course of the work. The authors also thank CAPT Norbert Elsner, USNR, for his technical encouragement throughout the course of the investigation. Special thanks are due to Dr. Murali Madhava, Chromalloy Division Oklahoma, for his technical assistance concerning the HIP processing and heat treatment of the material used in the study. The technical assistance of the authors colleagues at NRL, L.A. Cooley and J. R. Reed, in the metallographic aspects of this study is appreciated.

Table 1

DS-R80H Tensile and Creep/Rupture Specimen
Composition, Heat Treatment and HIP Processing Parameters

Composition
(Weight Percent)

Matl.	C	Mn	Si	Cr	W	Fe	Co	N	Mo	Al	Ti	Zr	Ni
455	.17	<.10	<.05	13.7	4.09	.04	9.14	2.27	3.86	3.03	4.90	.01	Bal.
491	.15	<.10	<.05	13.92	3.88	.03	9.28	2.28	4.00	2.91	4.95	.02	Bal.

Precipitation Heat Treatment (Bar Specimens)

Heat to 1190°C (2175°F) for 2 hours; cool to 1051°C (1925°F) and hold for 4 hours; cool to 871°C (1600°F) and age for 16 hours.

Precipitation Heat Treatment (HPT Blades)

Heat to 1190°C (2175°F) for 2 hours; cool to 1051°C (1925°F) and hold for 5 hours 20 minutes*; cool to 871°C (1600°F) and age for 16 hours.

HIP Processing Treatment

1200°C (2192°F) at 172.4 MPa (25 ksi) for 2 hours; cool at 50°C (90°F) per minute to 1038°C (1900°F); air cool to ambient.

* Includes additional 1 hr 20 min devoted to coating thermal cycle.

Table 2

TENSILE AND CREEP-RUPTURE PROPERTIES OF DS-R80H

TENSILE PROPERTIES (Not HIPPED)

Spec. No.	Temp.		Yield Stress		Ult. Stress		R.A./Elong. ⁽¹⁾ (%)
	(C)	(F)	(MPa)	(ksi)	(MPa)	(ksi)	
O491-1	982	1800	222.0	32.2	367.5	53.3	- /8.0
O491-2	982	1800	315.8	45.8	351.6	51.0	- /8.0
491	871	1600	556.4	80.7	844.6	122.5	28.4/ -
455	871	1600	471.6	68.4	1009.4	146.4	25.4/ -

CREEP-RUPTURE PROPERTIES

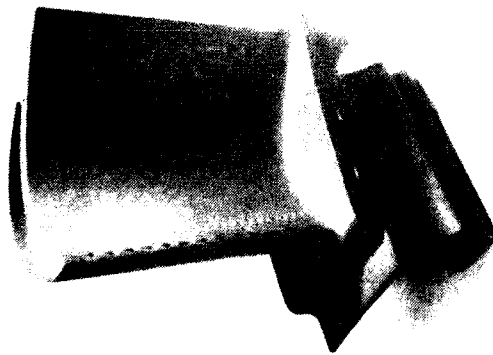
Spec. No.	Temp. Condition		Stress		Rupture Life (hours)	R.A./Elong. ⁽¹⁾ (%)
	(C)		(MPa)	(ksi)		
C491	871	Not HIPPED	351.6	51	304.5	42.1/18.2
R455-2	871	Not HIPPED	351.6	51	288.7	32.3/16.7
L491	982	Not HIPPED	206.8	30	56.9	63.7/26.5
P455-2	982	Not HIPPED	206.8	30	50.9	50.7/26.5
J491	871	Not HIP/HIP	351.6	51	269.6	16.9/13.7
E491	982	Not HIP/HIP	206.8	30	54.0	23.8/13.6
E455-2	871	HIPPED	351.6	51	163.5	35.5/21.8
N455-2	871	HIPPED	351.6	51	298.5	33.1/18.8
E455-1	982	HIPPED	206.8	30	27.1	59.0/23.4
N455-1	982	HIPPED	206.8	30	45.6	54.8/21.6

CREEP-RUPTRUE PROPERTIES OF MERL 72 WELD

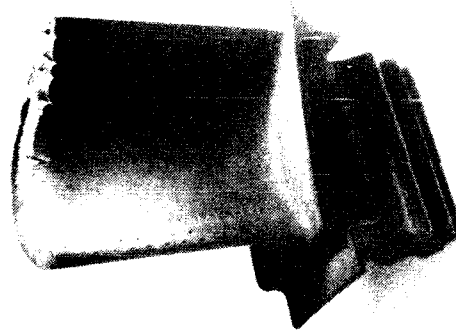
Spec. No.	Temp.		Stress		Rupture Life (hours)	R.A./Elong. ⁽¹⁾ (%)
	(C)	(F)	(MPa)	(ksi)		
S491-1	871	1600	351.6	51	1.3	46.1/16.1
S491-2	871	1600	275.8	40	14.5	40.2/16.9
W491	871	1600	227.5	33	43.0	36.3/15.3

⁽¹⁾Elongation was measured over a nominal 1.125 inch gage length.

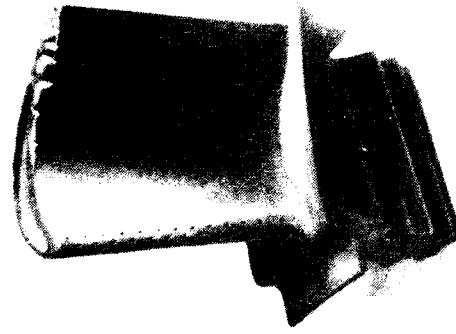
F404 HPT BLADES



NEW



LOW HRS.



HIGH HRS.

Figure 1. HPT blades in the new and engine-run conditions.

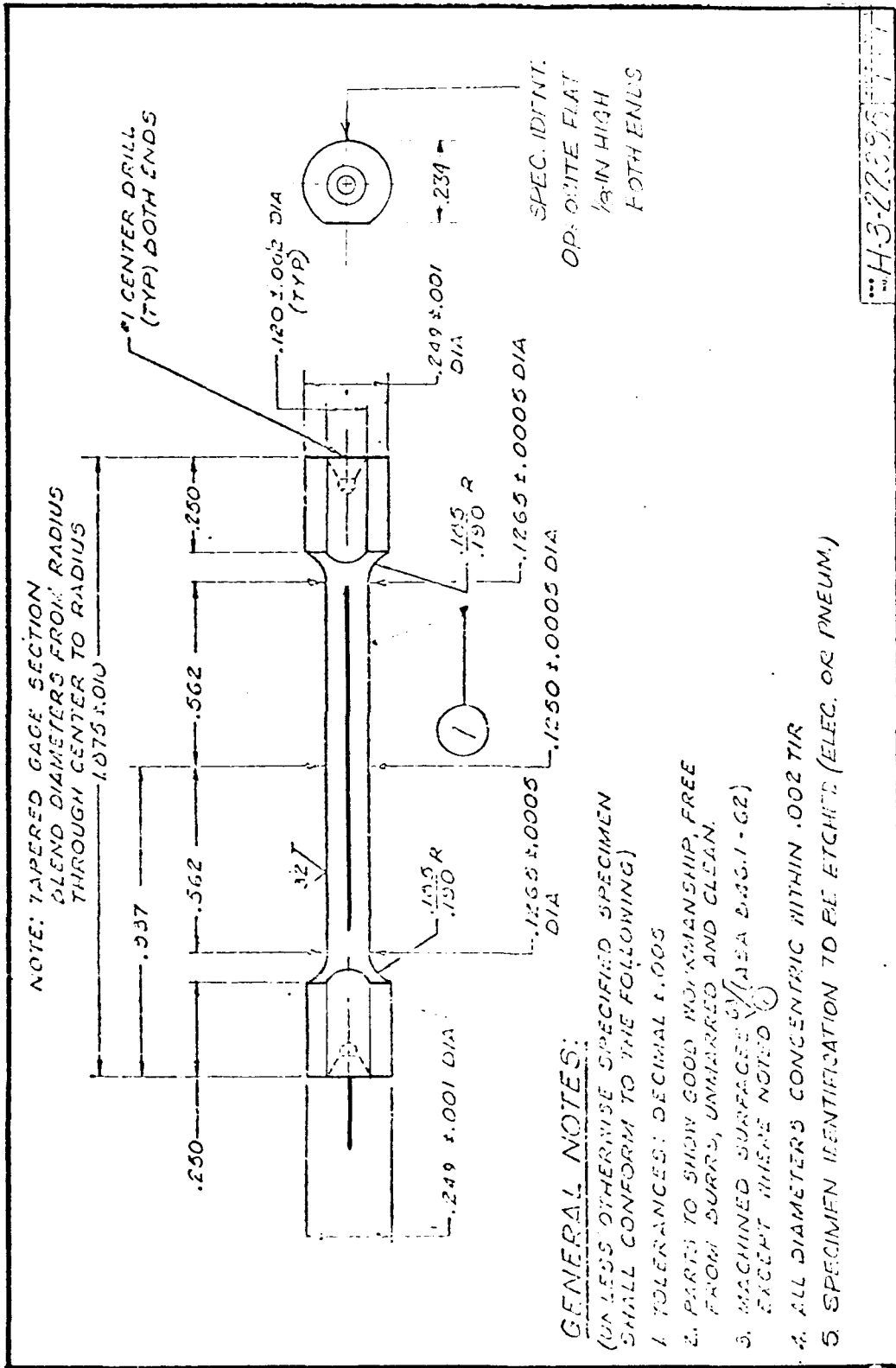


Figure 2. Tensile and creep-rupture specimen details.

DIRECTIONALLY SOLIDIFIED RENE' 80H

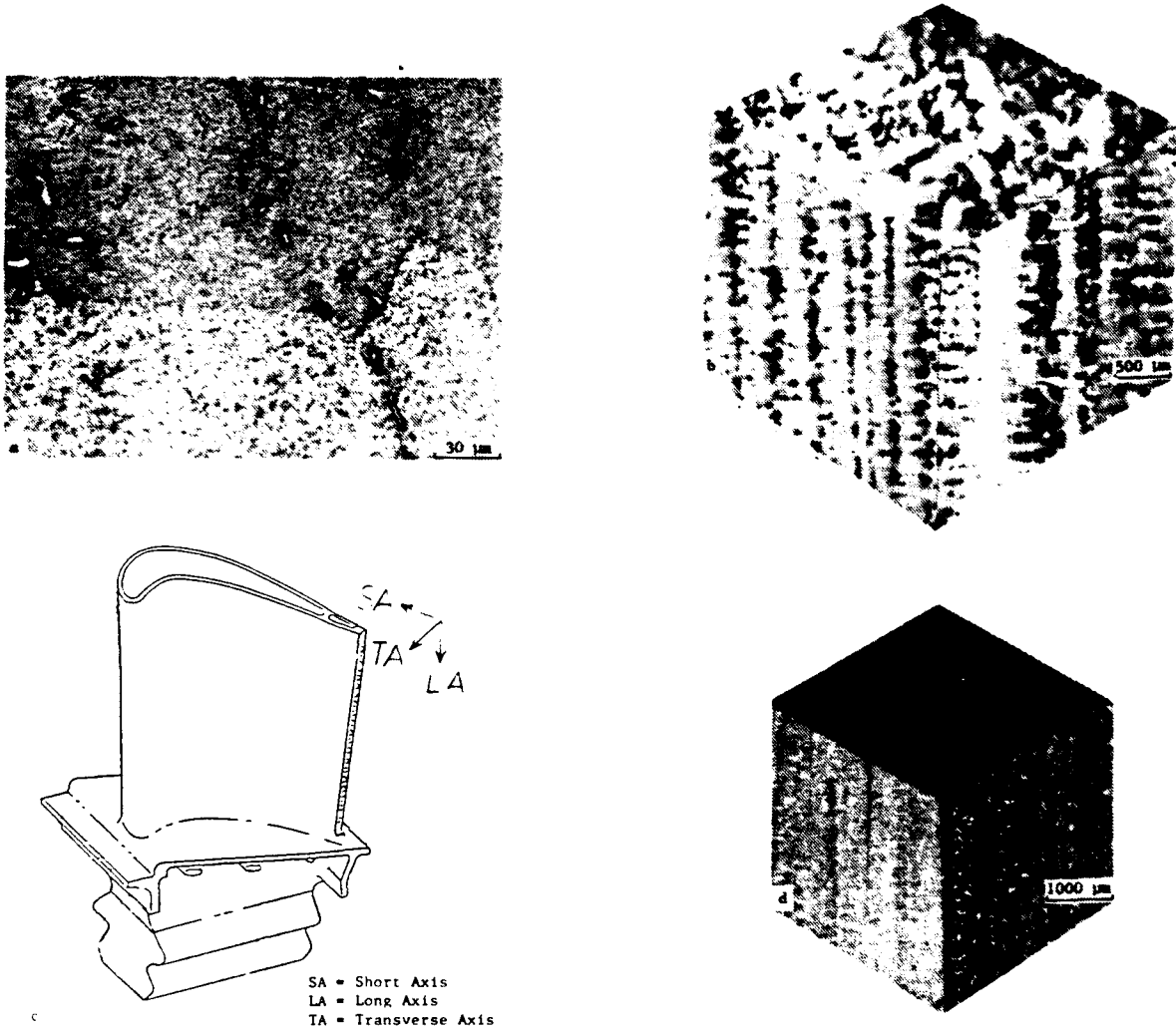


Figure 3. Optical microstructure of DS-R80H blade alloy showing columnar grain structure.

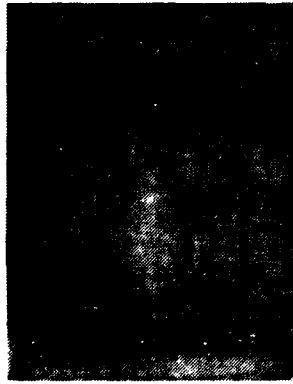
DS RENE' 80H

Non-HIPPED F404 BLADES

TIP REGION



NEW



LOW HRS.

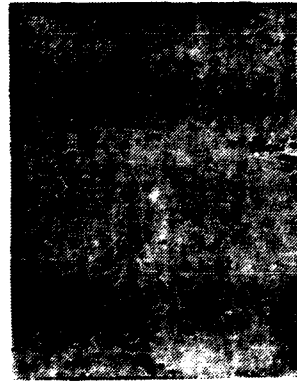


HIGH HRS.

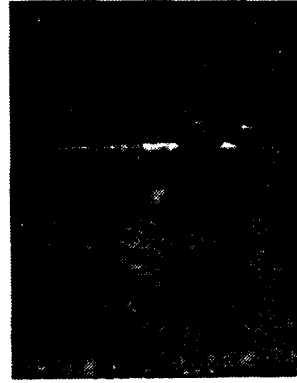
MID REGION



NEW



LOW HRS.



HIGH HRS.

Figure 4. Optical micrographs of new and engine run (not HIP) DS-R80H blades at two locations along the blade axis.

DS RENE' 80H



**NEW BLADE
NOT HIPPED**



**CREEP SPECIMEN
NOT HIPPED**

Figure 5. Transmission electron micrographs of gamma prime precipitates in new DS-R80H blade and in new creep test specimen.

DS RENE' 80H

F404 BLADES - MID REGION

Non-HIPPED



NEW



LOW HRS.

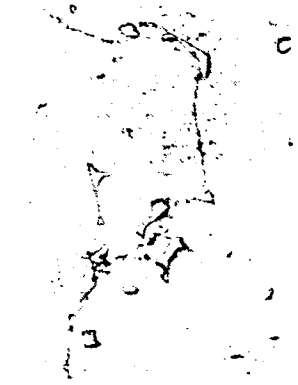


HIGH HRS.

HIPPED



NEW



LOW HRS.



HIGH HRS.

Figure 6. Optical micrographs of the mid region of HPT blades in new, low hours and high hours engine run conditions for the HIP processed and non-HIP processed conditions.

DS RENE' 80H

F404 BLADES - TIP REGION

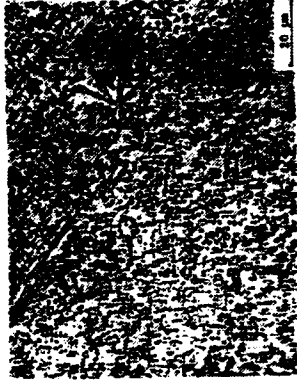
Non-HIPPED



NEW



LOW HRS.



HIGH HRS.

HIPPED



NEW



LOW HRS.



HIGH HRS.

Figure 7. Optical micrographs of the tip region of HPT blades in new, low hours and high hours engine run conditions for the HIP processed and non-HIP processed conditions.

**DS RENE' 80H
F404 BLADES**

LOW HRS BLADES



NOT HIPPED



HIPPED

HIGH HRS BLADES



NOT HIPPED

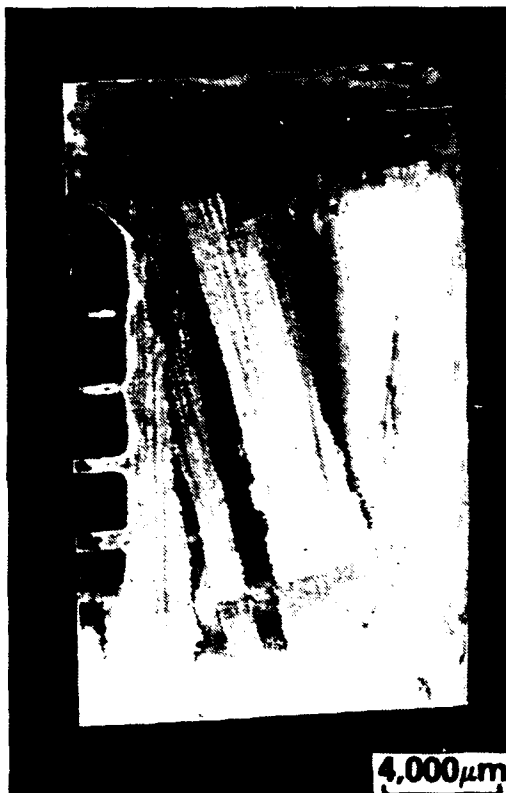


HIPPED

Figure 8. Transmission electron micrographs of the gamma prime precipitates in the tip region of the low and high hours engine run blades.

DS RENE' 80H F404 BLADES—TIP REPAIR

INTERIOR—EXTERIOR SURFACES



INTERIOR SURFACE



EXTERIOR SURFACE

Figure 9. Optical micrographs of the interior and exterior surfaces of DS-R80H blades which have received a MERL 72 tip repair.

DS RENE' 80H
F404 BLADES-TIP REPAIR

BLADE SECTIONS

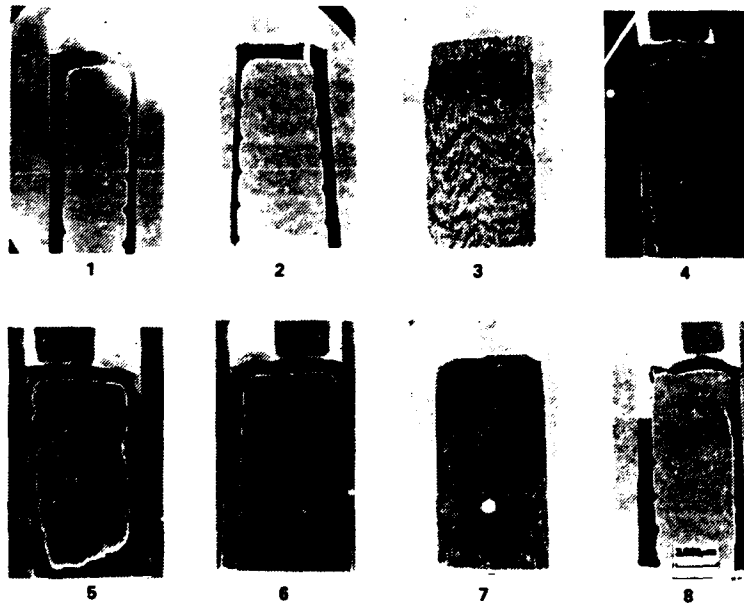
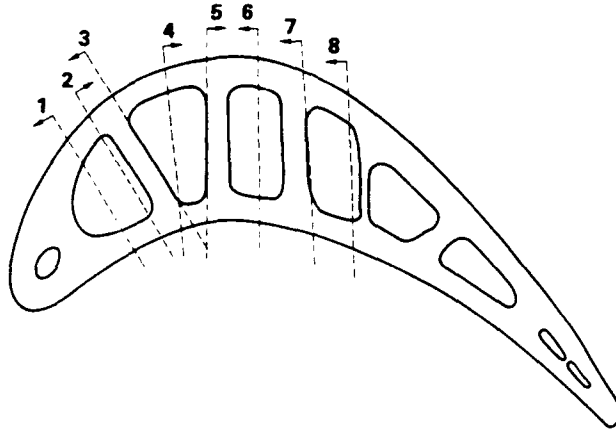


Figure 10. Section views of the microstructure of a DS-R80H blade illustrating the blade-weld interface through the blade cross-section.

**DS RENE' 80H
F404 BLADES—TIP REPAIR**

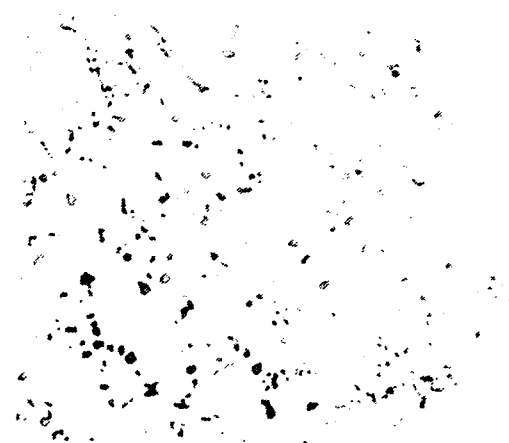


a

BLADE—WELD



b



c

WELD FUSION ZONE

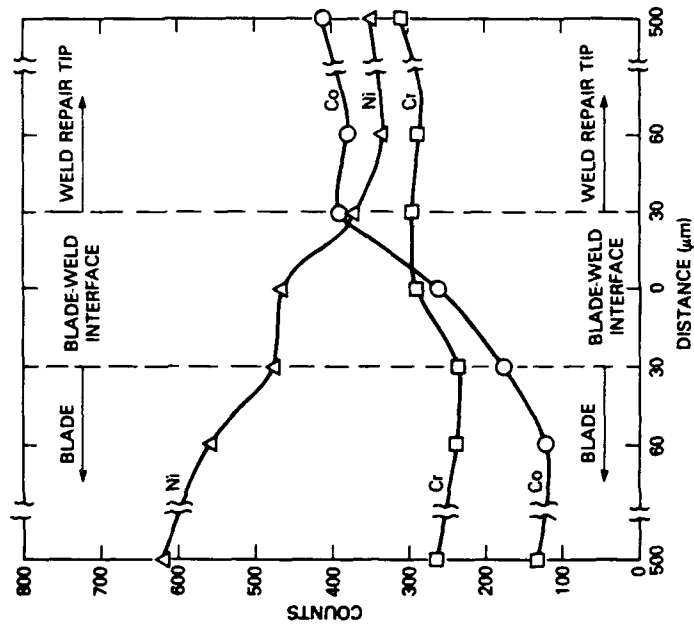
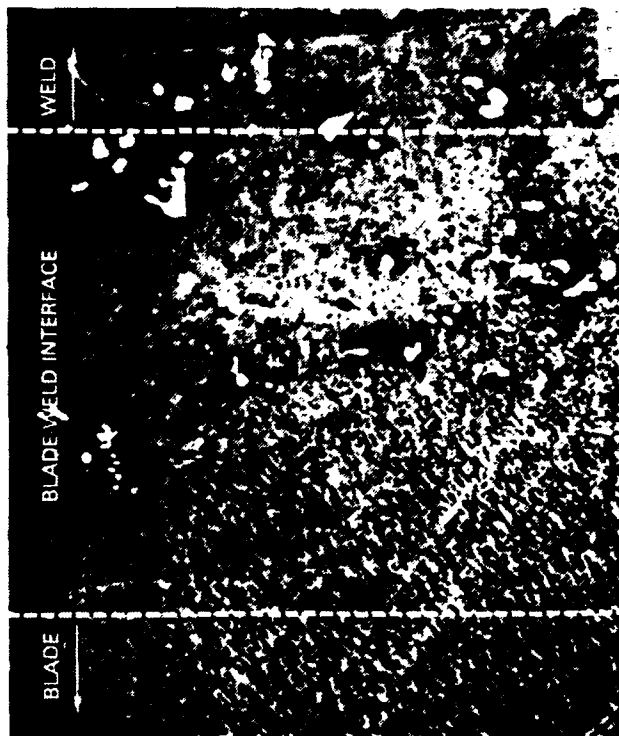


d

WELD

Figure 11. Optical micrographs of the blade-weld interface.

MICROSTRUCTURE AND COMPOSITION OF DS-R80-H BLADE/MERL 72 WELD INTERFACE



BLADE-WELD INTERFACE MICROSTRUCTURE

COMPOSITION PROFILES

Figure 12. Microstructure of the blade-weld interface region and composition profiles detailing the Co, Ni and Cr gradients through the interface.

MICROSTRUCTURE OF DS-R80-H BLADE/MERL 72 TIP REPAIR

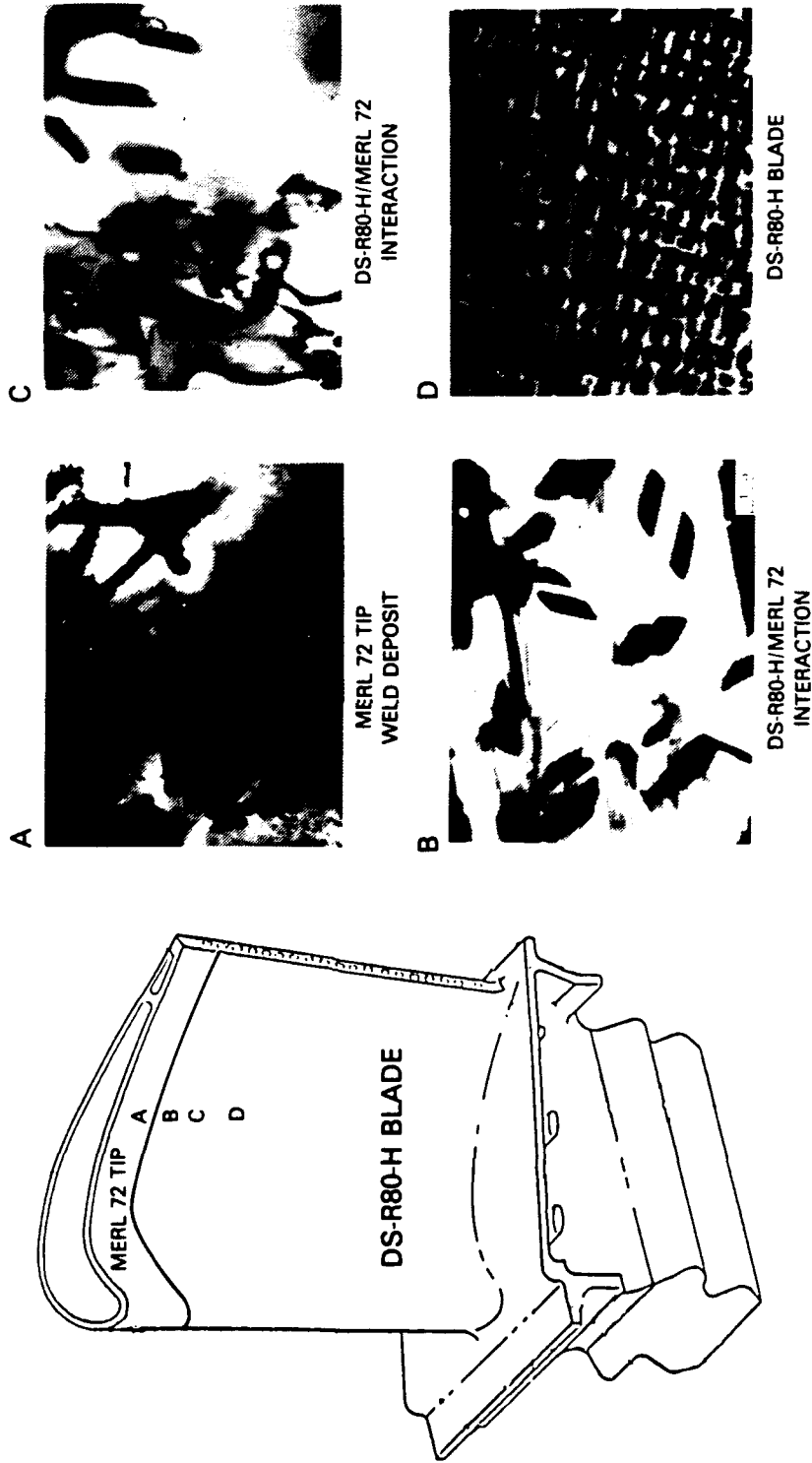


Figure 13. Transmission electron micrographs of the blade-weld interface region showing the change in the precipitate microstructure with location relative to the interface.

DS-R80H HPT BLADES, F404 ENGINE
ASMET ENGINE TESTED

TRAILING EDGE TIP REGION

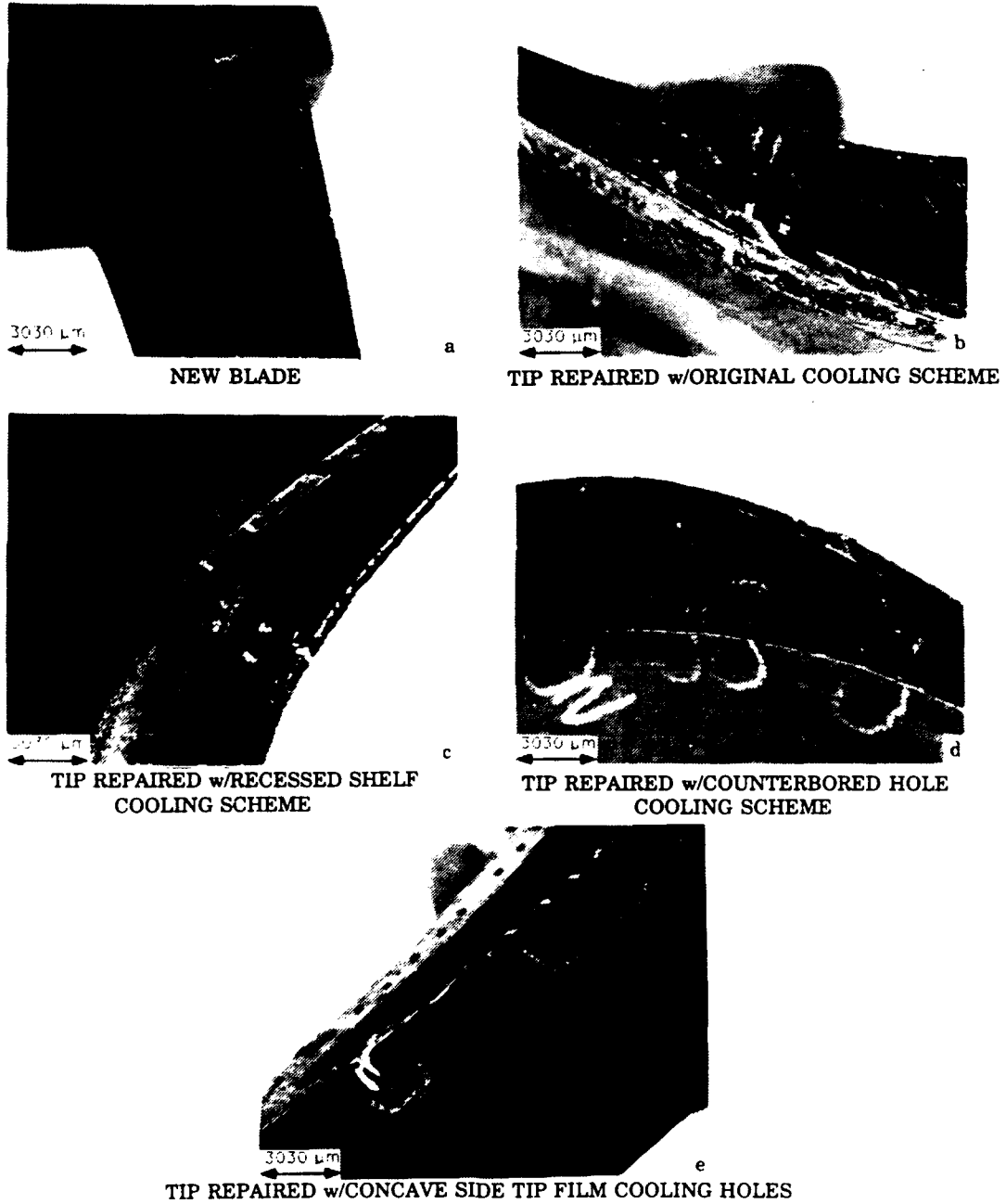


Figure 14. Trailing edge tip regions of ASMET engine tested, MERL 72 tip repaired, DS-R80H HPT blades.

DS-R80H HPT BLADE, F404 ENGINE
ASMET ENGINE TESTED

NEW BEFORE ENGINE TEST

SECTION THROUGH TRAILING EDGE

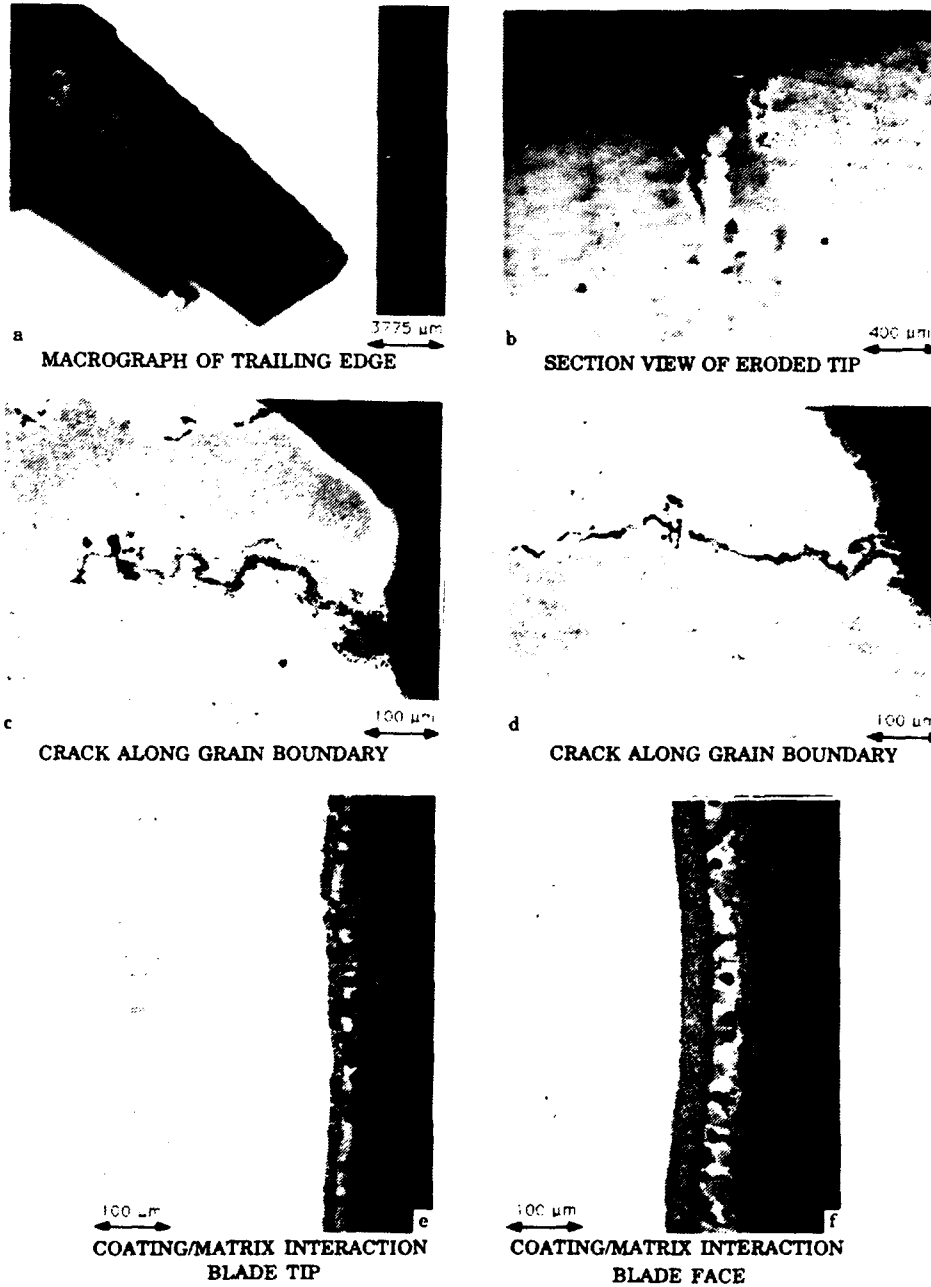


Figure 15. DS-R80H HPT blade, ASMET engine tested, new before test.

DS-R80H HPT BLADE, F404 ENGINE
ASMET ENGINE TESTED

CHROMALLOY TIP REPAIRED TO ORIGINAL TIP
COOLING SCHEME BEFORE ENGINE TEST

SECTION THROUGH BLADE

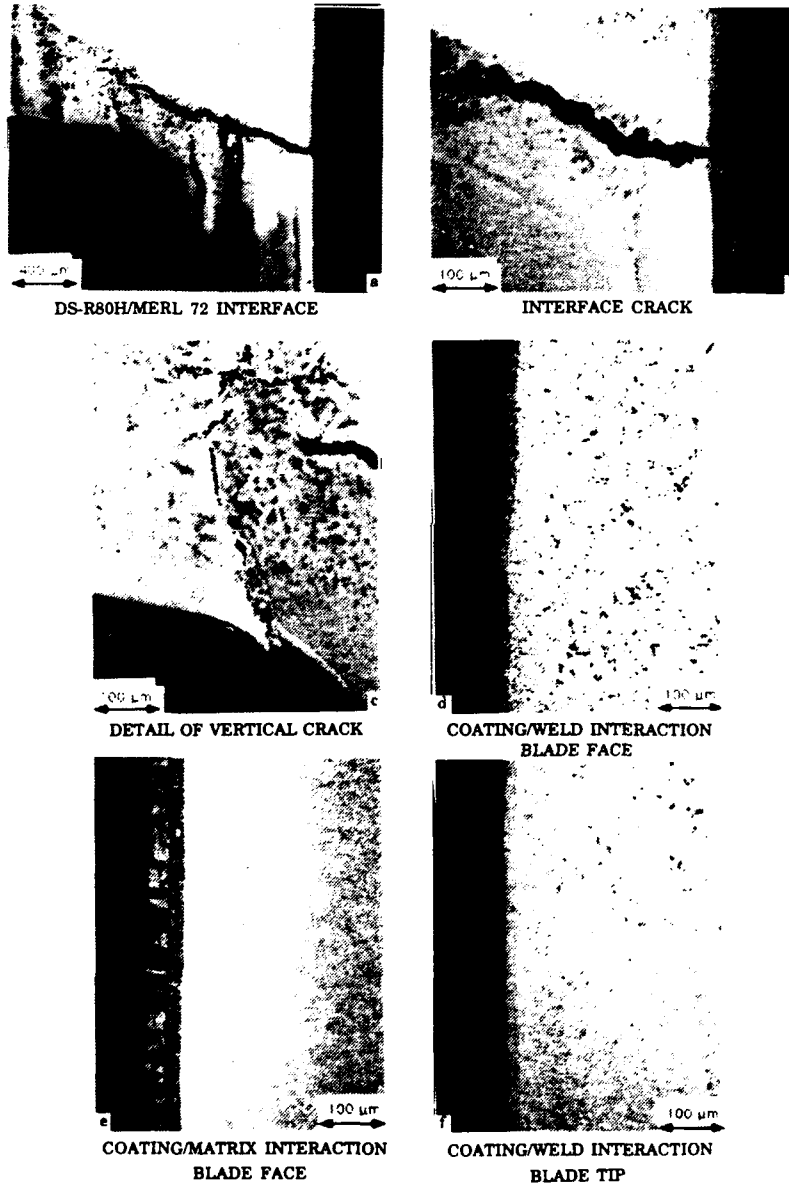


Figure 16. DS-R80H HPT Blade, ASMET engine tested, MERL 72 tip repaired by Chromalloy to original tip cooling scheme before engine test.

DS-R80H HPT BLADE, F404 ENGINE
ASMET ENGINE TESTED

CHROMALLOY TIP REPAIRED TO ORIGINAL TIP
COOLING SCHEME BEFORE ENGINE TEST

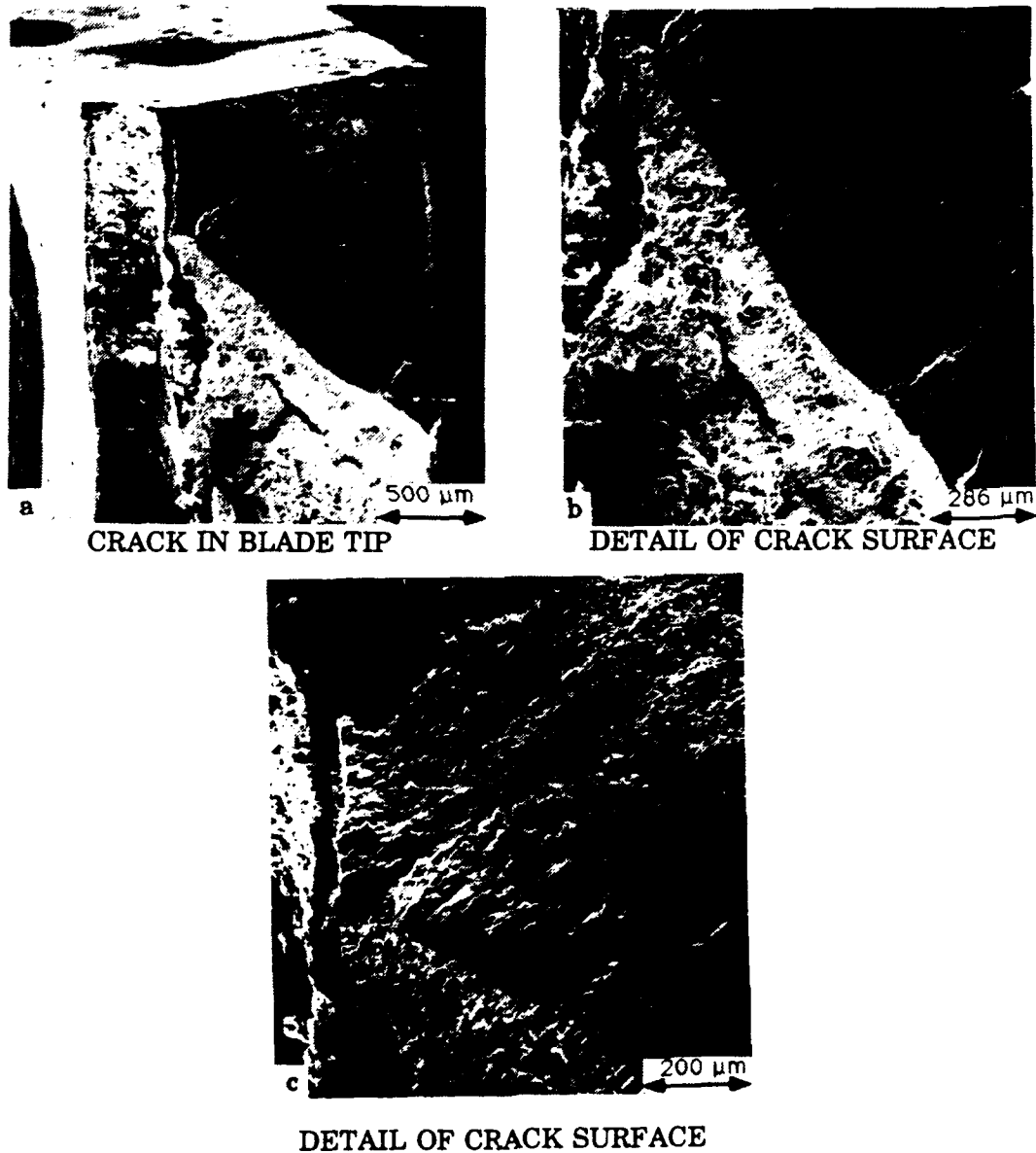


Figure 17. Fractographs of tip cracks formed during the ASMET engine test of a repaired blade with the original tip cooling scheme before test.

**DS-R80H HPT BLADE, F404 ENGINE
ASMET ENGINE TESTED**

**CHROMALLOY TIP REPAIRED w/RECESSED SHELF
TIP COOLING SCHEME BEFORE ENGINE TEST**

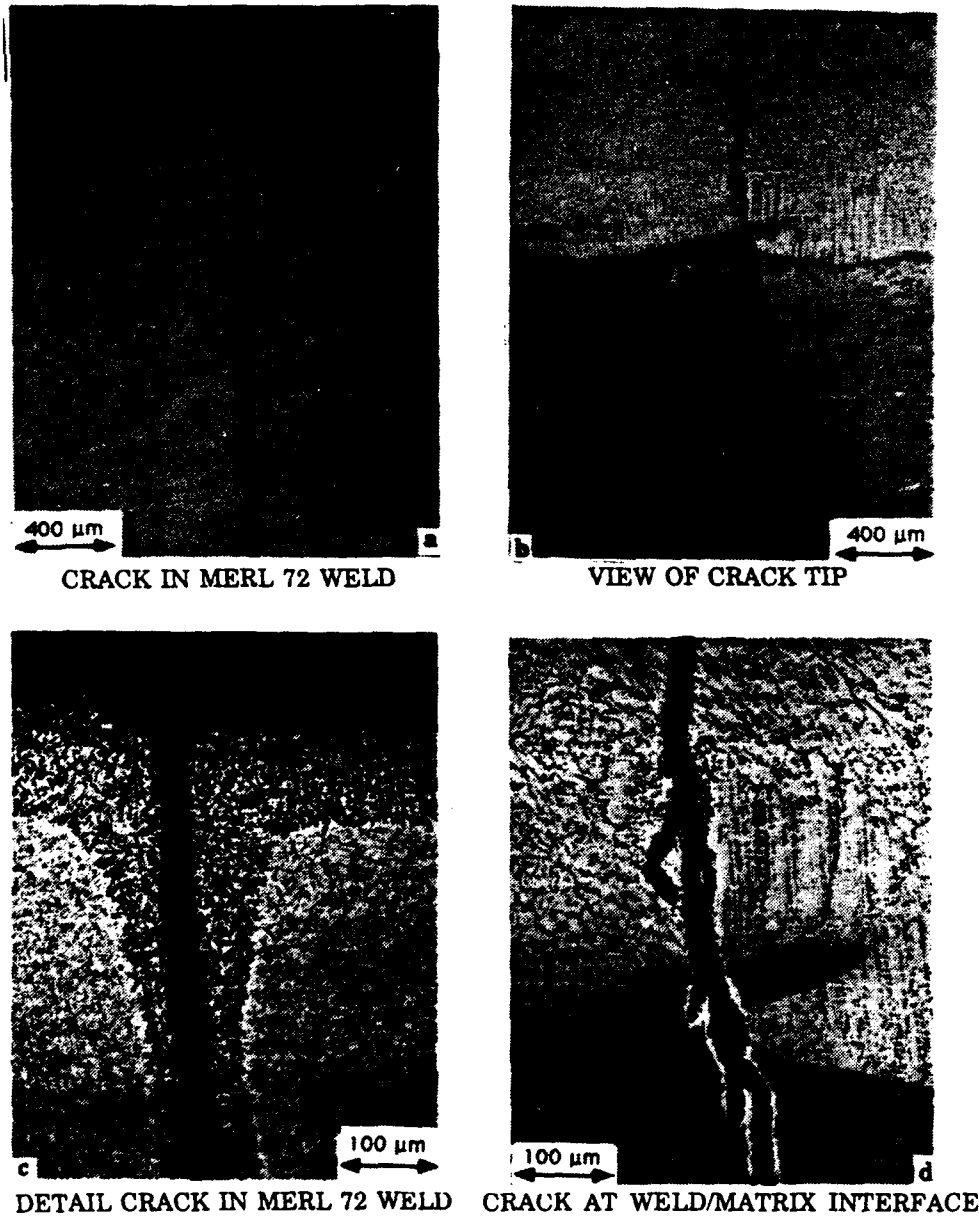


Figure 18. DS-R80H HPT blade, ASMET engine tested, MERL 72 tip repaired by Chromalloy with recessed shelf tip cooling scheme before engine test.

DS-R80H HPT BLADE, F404 ENGINE
ASMET ENGINE TESTED

CHROMALLOY TIP REPAIRED w/COUNTERBORED
TIP COOLING HOLES BEFORE ENGINE TEST

CRACK FORMATION AT COOLING HOLES

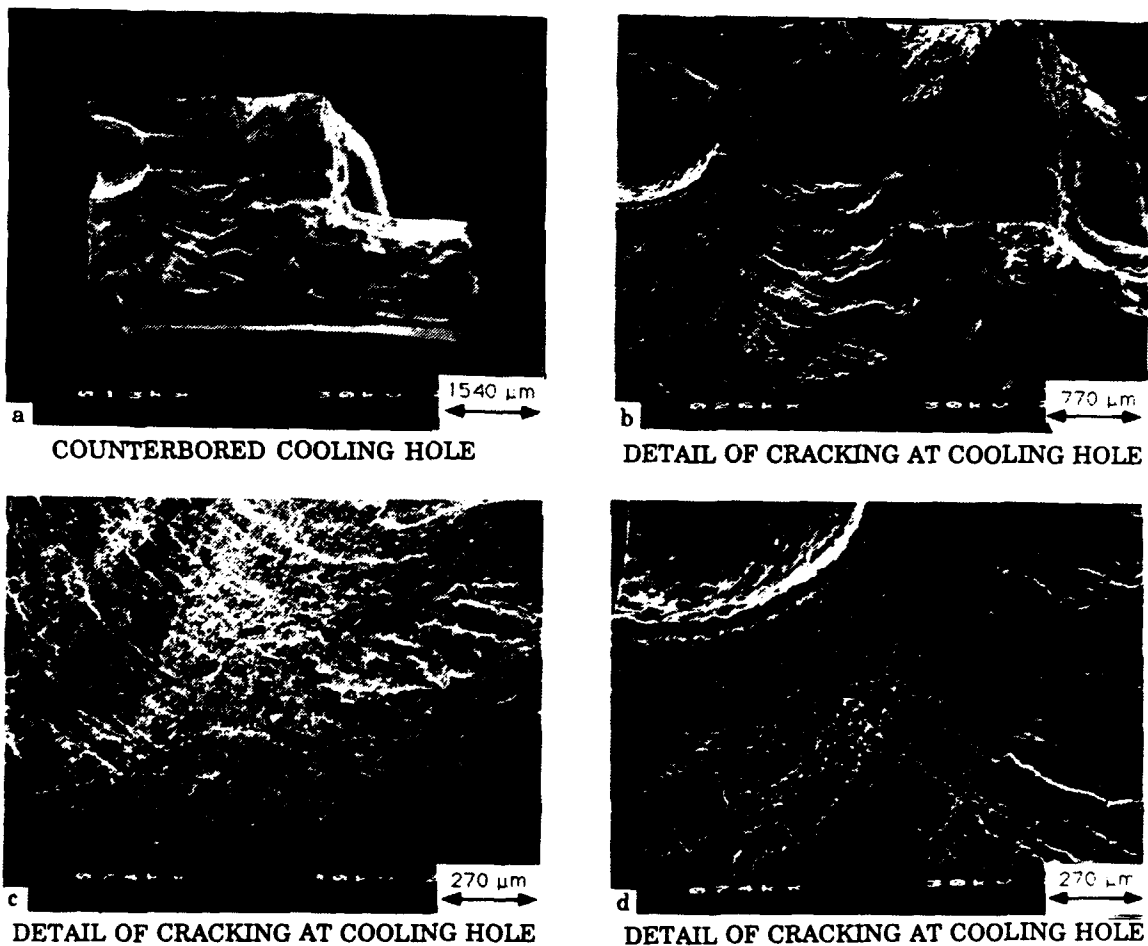


Figure 19. Fractographs of a crack in a DS-R80H HPT blade, ASMET engine tested, MERL 72 tip repaired by Chromalloy with counterbored tip cooling holes before engine test.

**DS-R80H HPT BLADE, F404 ENGINE
ASMET ENGINE TESTED**

**CHROMALLOY TIP REPAIRED w/CONCAVE
SIDE TIP FILM COOLING HOLES BEFORE
ENGINE TEST**

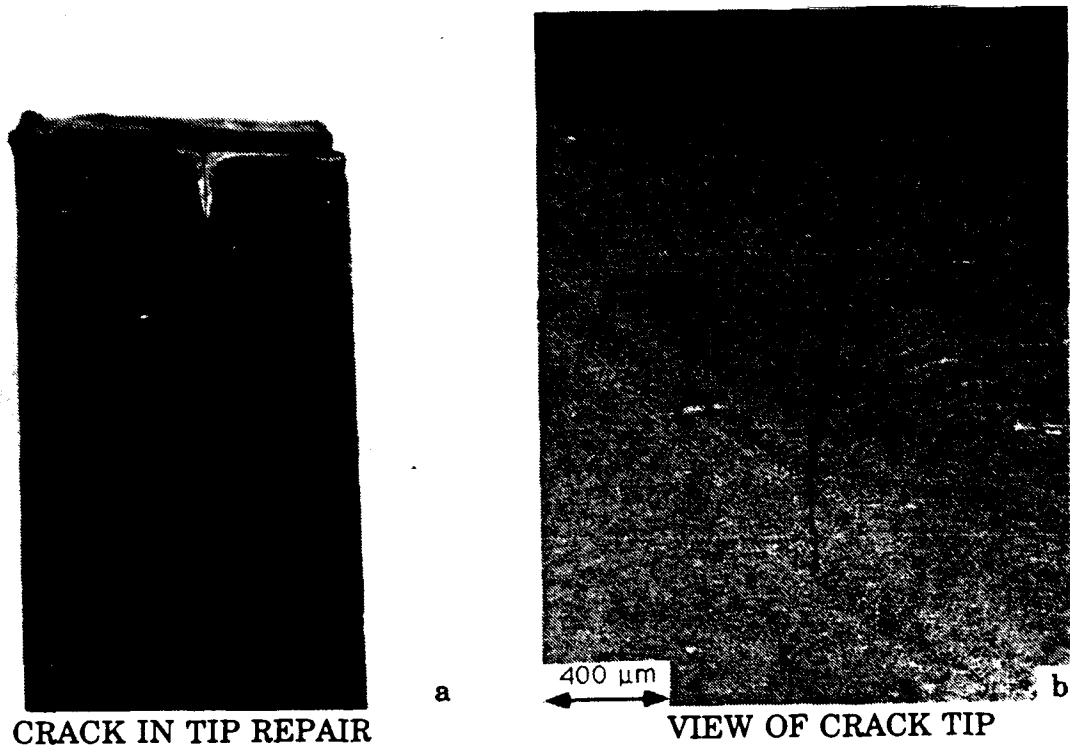


Figure 20. Photomicrographs of tip cracks formed during the ASMET engine test of a blade repaired with concave side tip film cooling hole scheme.

**DS-R80H HPT BLADE, F404 ENGINE
ASMET ENGINE TESTED**

**CHROMALLOY TIP REPAIRED w/CONCAVE
SIDE TIP FILM COOLING HOLES BEFORE
ENGINE TEST**

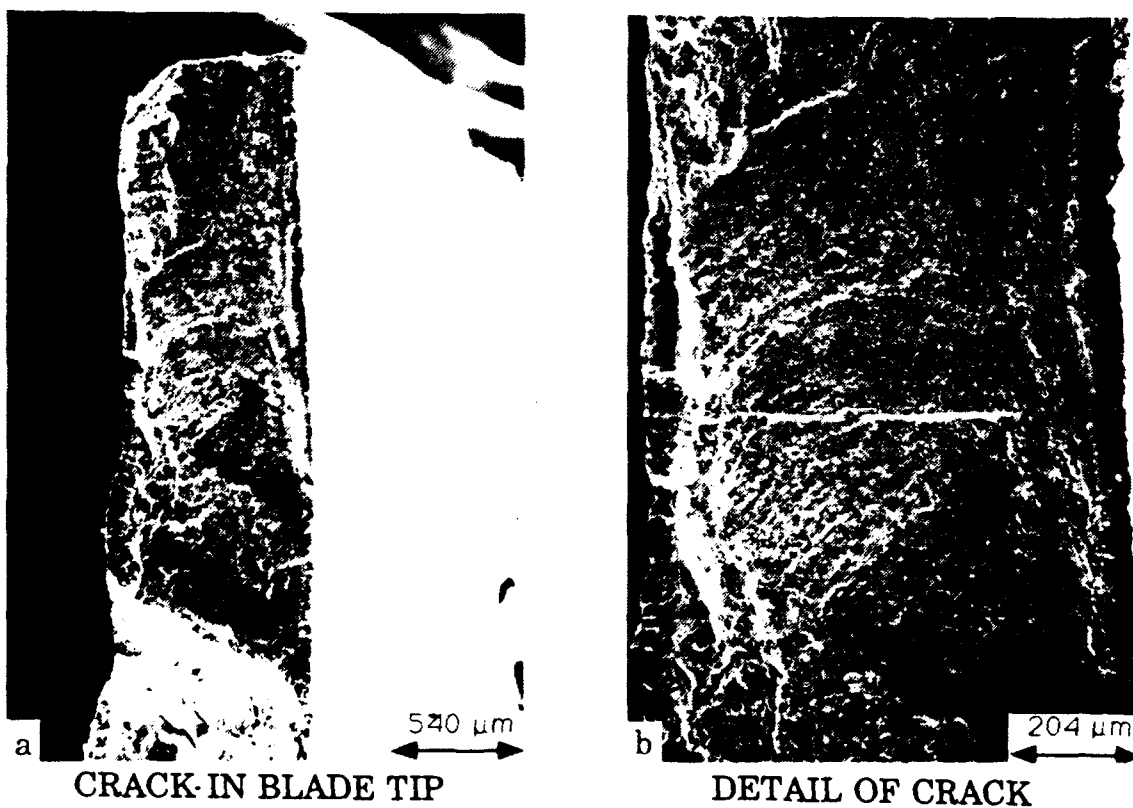


Figure 21. Fractographs of a crack in a DS-R80H HPT blade, ASMET engine tested, MERL 72 tip repaired by Chromalloy with concave side tip film cooling holes before engine test.

ASMET ENGINE TESTED BLADE BLADE/WELD COMPOSITION PROFILES

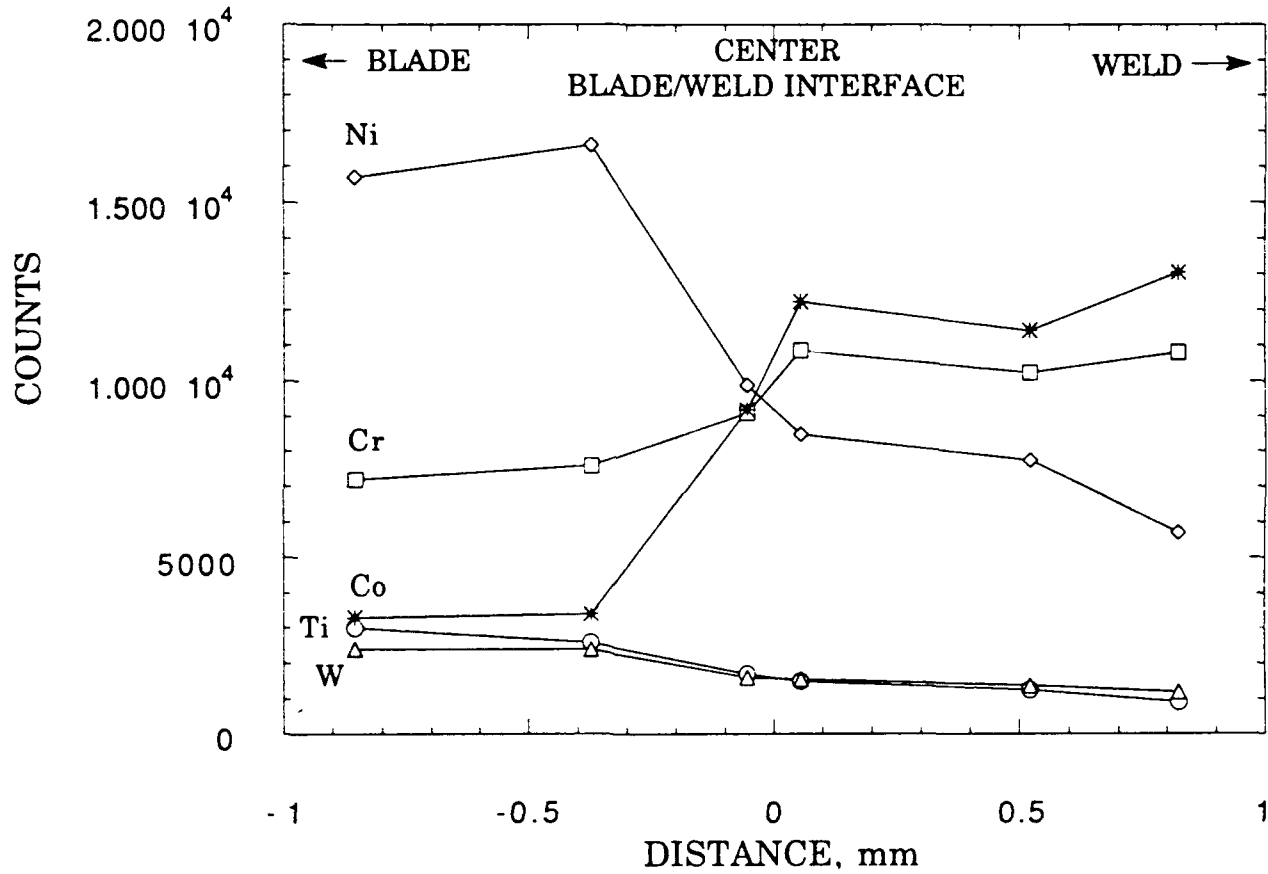


Figure 22. Semi-quantitative compositional analysis of the DS-R80H blade/MERL 72 weld interface region of an ASMET engine tested blade.

DS RENE' 80H

CREEP TEST SPECIMENS

Non-HIPPED



HIPPED



Figure 23. Optical microstructure of the not-HIP and HIP processed creep-rupture specimens.

DS-R80H CREEP-RUPTURE BEHAVIOR

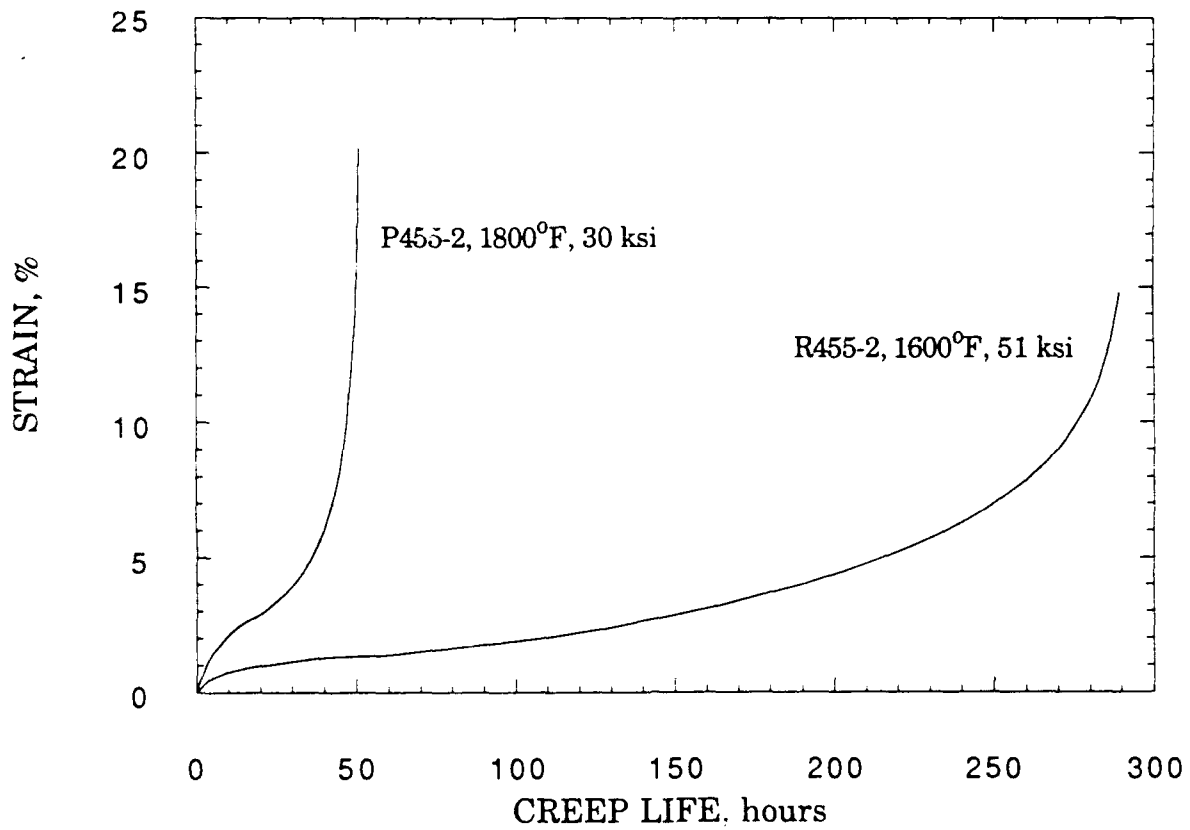


Figure 24. Creep-rupture results for not-HIP processed DS-R80H tested at 871 and 982°C.

DS-R80H CREEP-RUPTURE BEHAVIOR

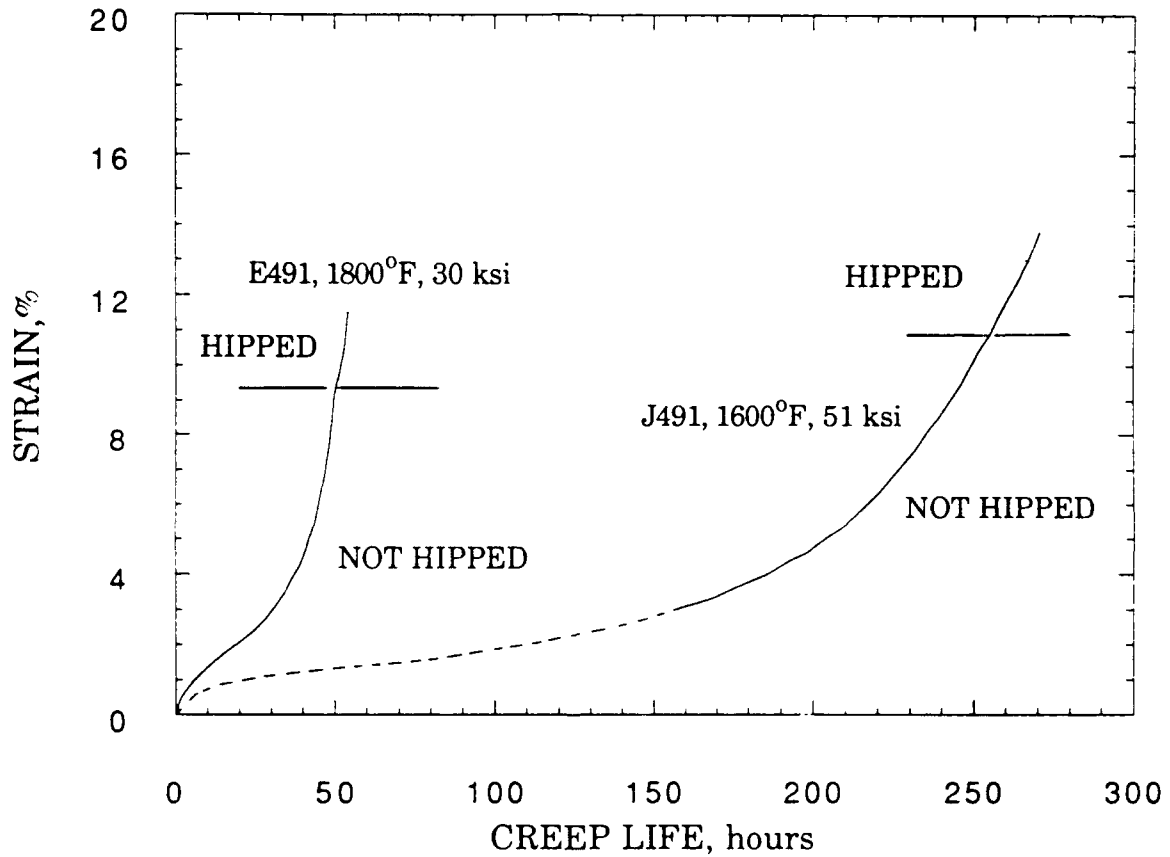
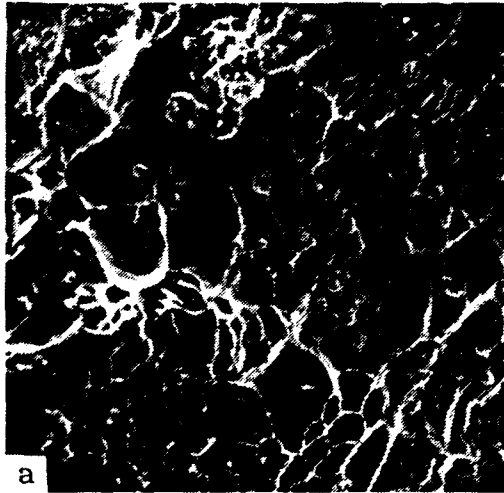
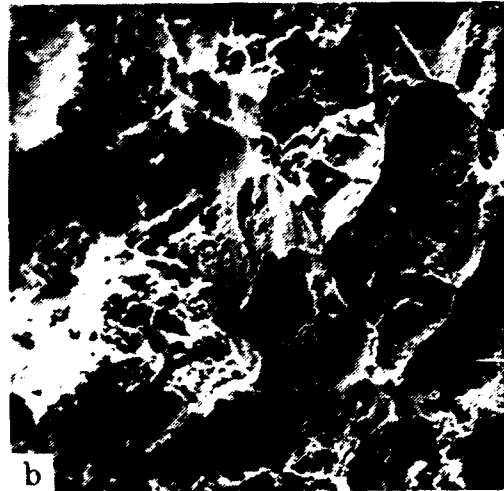


Figure 25. Creep-rupture results for not-HIP processed DS-R80H tested at 871 and 982°C.

**DS RENE' 80H
CREEP FRACTURE SURFACES
NOT HIP PROCESSED**

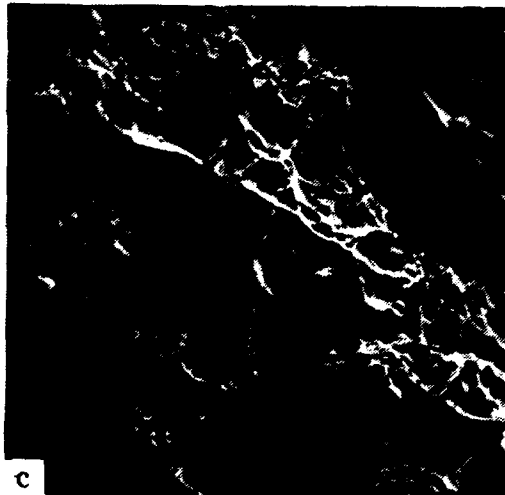


871°C, 51 ksi

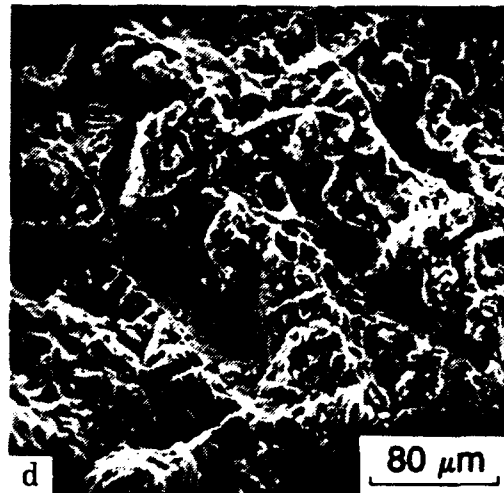


982°C, 30 ksi

HIP PROCESSED



871°C, 51 ksi

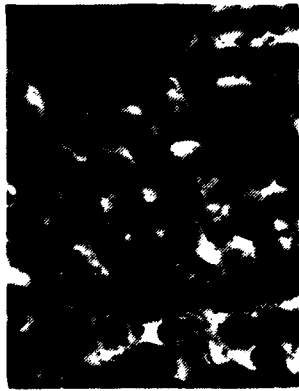


982°C, 30 ksi

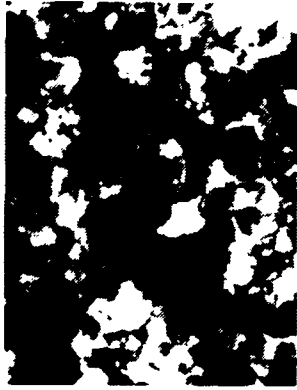
Figure 26. Scanning electron micrographs of the DS-R80H creep-rupture specimens tested at 871 and 982°C.

DS RENE' 80H CREEP TEST SPECIMEN MICROSTRUCTURE

871°C (1600°F) TEST TEMPERATURE



NOT HIP PROCESSED



HIP PROCESSED

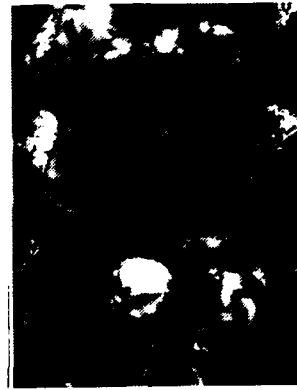


NOT HIP/HIP PROCESSED

982°C (1800°F) TEST TEMPERATURE



NOT HIP PROCESSED



HIP PROCESSED



NOT HIP/HIP PROCESSED

Figure 27. Transmission electron micrographs of the creep-rupture specimens tested at 871 and 982°C.

MERL 72 WELD ALLOY CREEP SPECIMENS

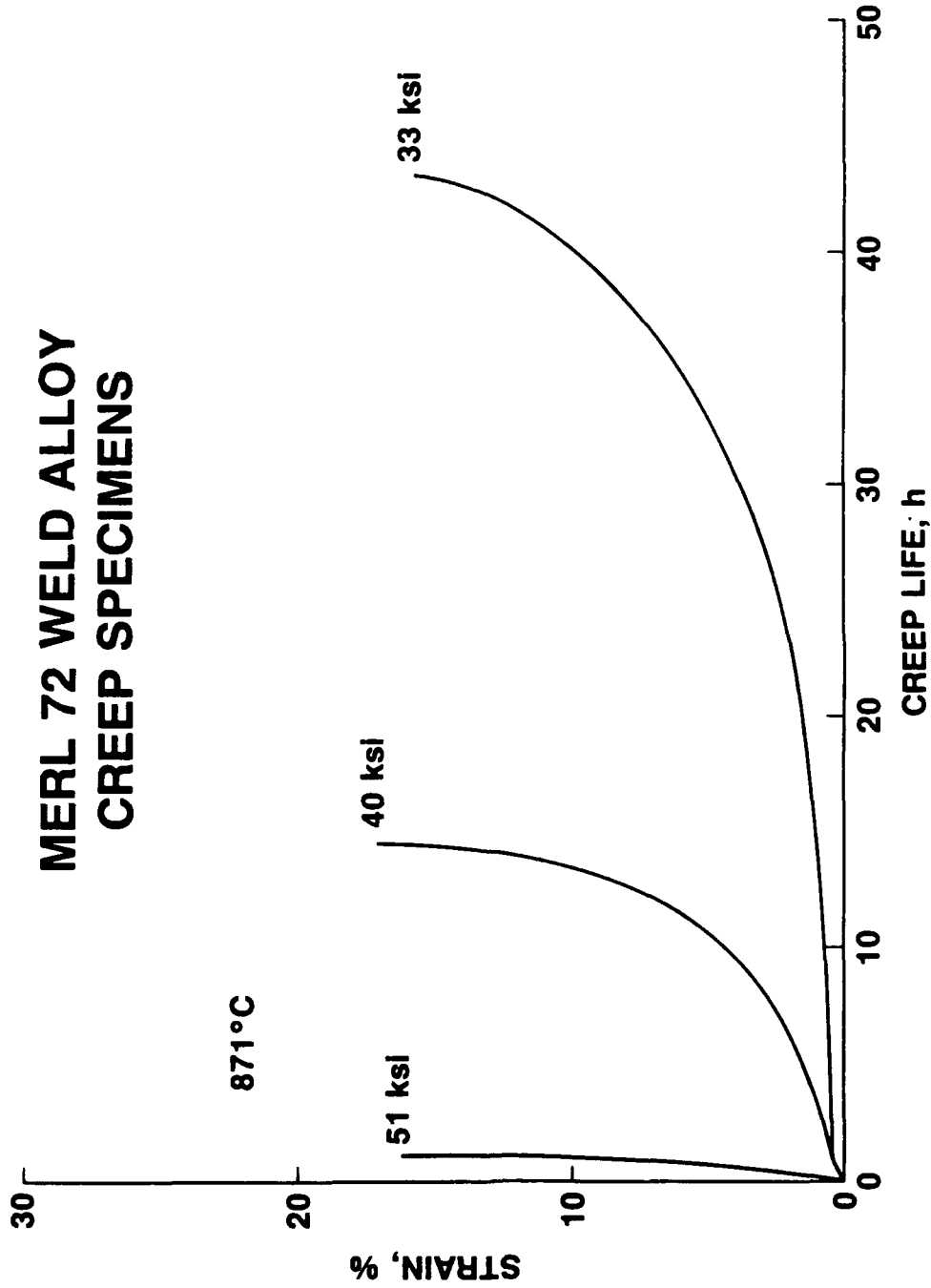


Figure 28. DS-R80H/MERL 72/DS-R80H creep-rupture test specimens illustrating both untested and tested specimens. Note the neck formed in the tested specimen indicative of the ductility of the weld material.

DSR80H—MERL 72 SPECIMENS

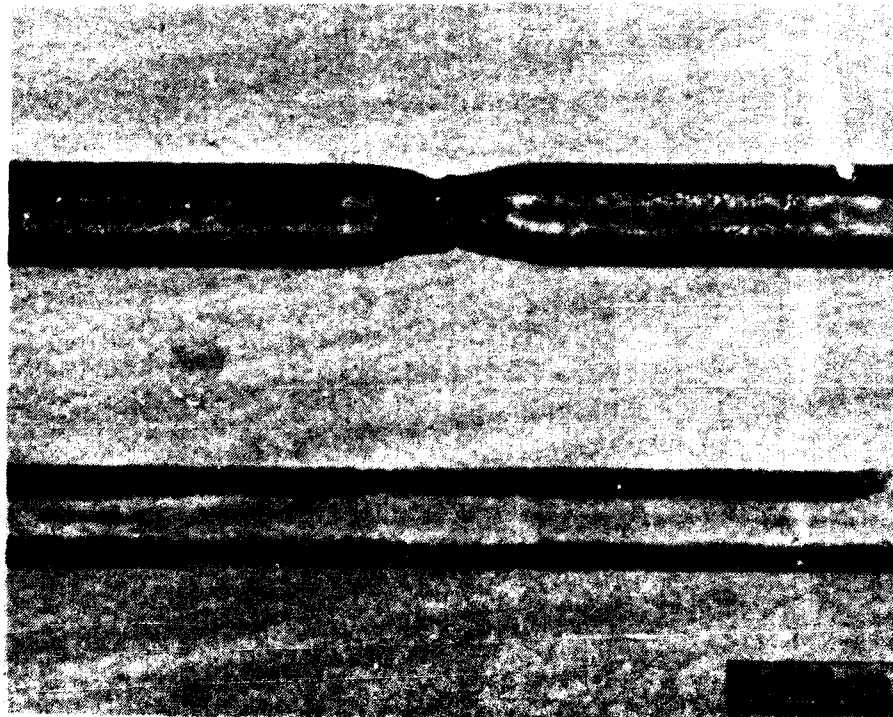
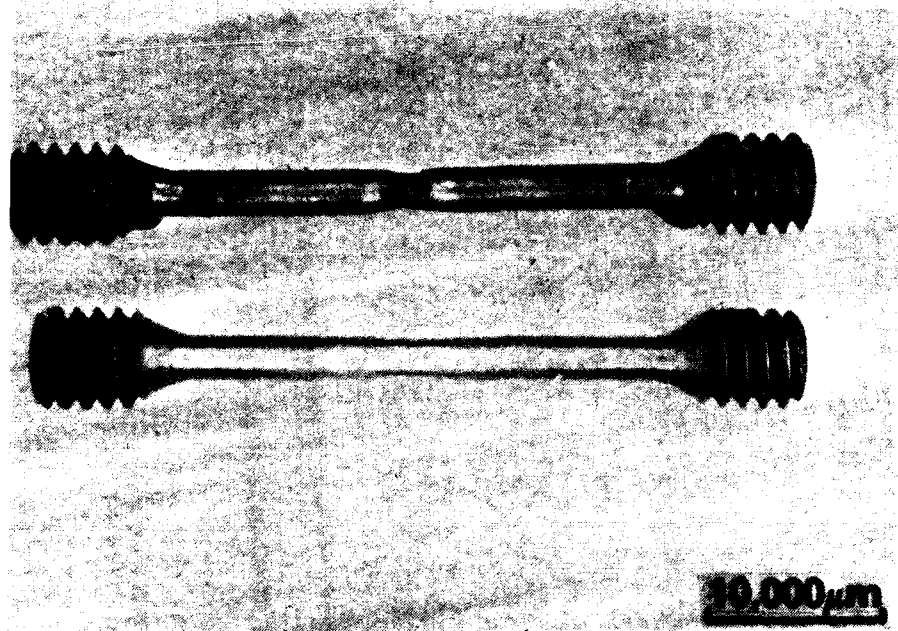
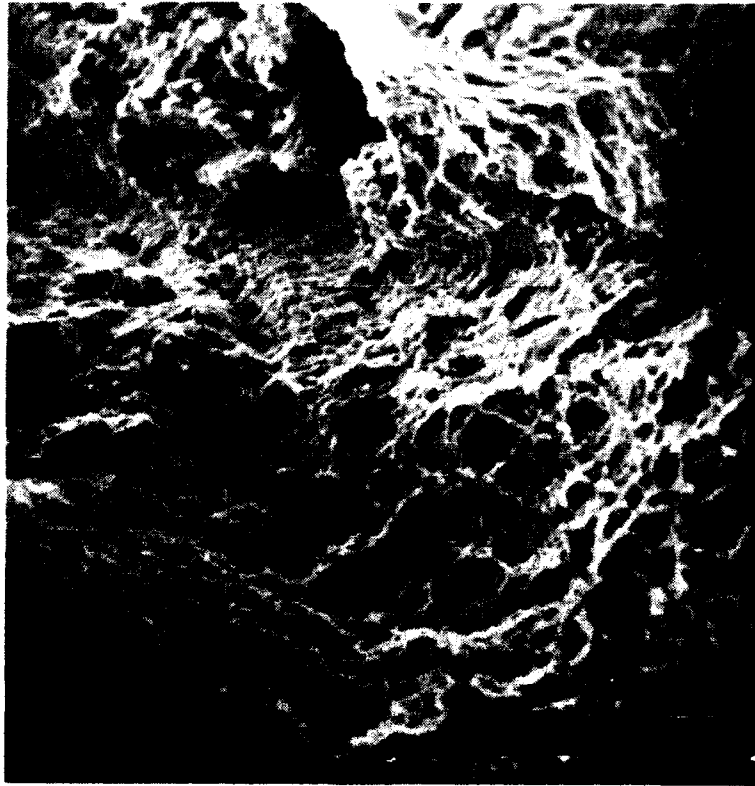
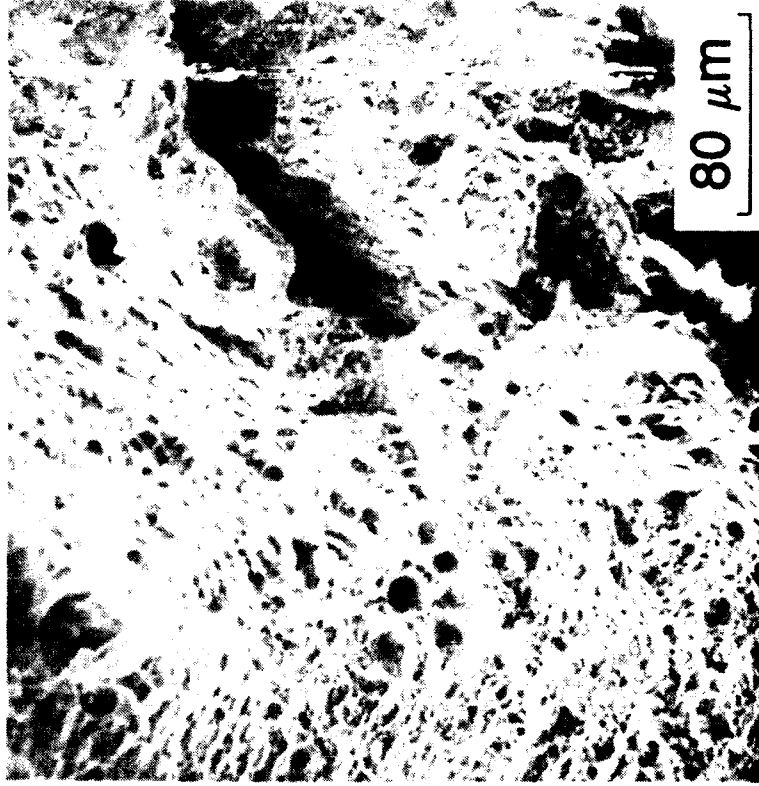


Figure 29. Creep-rupture results for DS-R80H/MERL 72/DS-R80H specimens tested at 871°C.

MERL 72 CREEP FRACTURE SURFACES



871°C, 30 ksi



871°C, 51 ksi

Figure 30. Scanning electron micrographs of the creep fracture surfaces of MERL 72.